Materials Today Advances 8 (2020) 100119

Contents lists available at ScienceDirect

Materials Today Advances

journal homepage: www.journals.elsevier.com/materials-today-advances/

Engineering ferrite nanoparticles with enhanced magnetic response for advanced biomedical applications

Y. Wang [a], Y. Miao [b], G. Li [a], M. Su [a], X. Chen [b], H. Zhang [b], Y. Zhang [b], W. Jiao [b], Y. He [b], J. Yi [c], X. Liu [a], H. Fan [a, b, *]

[a] Key Laboratory of Resource Biology and Biotechnology in Western China, Ministry of Education, School of Medicine, Northwest University, Xi'an, 710069, China
[b] Key Laboratory of Synthetic and Natural Functional Molecule Chemistry of the Ministry of Education, College of Chemistry and Materials Science, Northwest University, Xi'an, 710127, China
[c] Global Innovative Centre for Advanced Nanomaterials, School of Engineering, The University of Newcastle, Callaghan, 2308, New South Wales, Australia

ARTICLE INFO

Article history:
Received 5 August 2020
Received in revised form
14 October 2020
Accepted 18 October 2020
Available online 13 December 2020

Keywords:
Magnetic ferrite nanoparticles
MR signal amplification
Magnetothermal response
Magnetomechanical response
Biomedical materials

ABSTRACT

One of the most attractive features of magnetic ferrite nanoparticles (MFNPs) in biomedical application is that they can mediate external magnetic field to produce local magnetic field, magnetic thermal and magnetic force effects. These generated effects can later be utilized in the diagnosis and treatment of various diseases. The application performance is mainly determined by the nano-magnetism of MFNPs. Therefore, by modulating the magnetic properties, the improved magnetic resonance (MR) signals, magnetothermal, and magnetomechanical effects of the MFNPs can be achieved. In this review, we summarize the strategies used in the engineering of MFNPs to enhance MR imaging sensitivity and magnetic thermal conversion efficiencies. We will also discuss the detailed magnetoresponsive mechanism arising from the critical magnetic properties of MFNPs. Furthermore, we will highlight the recent progresses of the engineered MFNPs in biomedical applications, with emphasis in MR signal amplification, magnetothermal, and magnetomechanical response in biomedical applications.

1. Introduction

Since ancient Greek time, lodestone, *i.e.*, bulk magnetite (Fe_3O_4), has been used in the treatment of common ailments. With the advancement in nano-biotechnology, the applications of such magnetic ferrite nanoparticles (MFNPs) have evolved, which extends to the modern biomedicine and clinical study [1–7]. As biological tissues are transparent to magnetic fields, the most attractive advantage of MFNPs in biomedical applications is that they can complete various functions triggered by invisible, tissue-penetrating magnetic field [8,9]. For instance, natural magnetotactic bacteria build iron oxide nanoparticles (IONPs) in a chain configuration to generate a permanent dipole in their cells so as to navigate toward their favorable habitats by sensing the Earth's magnetic field [10]. These MFNPs possess good biocompatibility, which have already been used as imaging and therapeutic agents in preclinical and clinical settings [2,3,11]. As a result of the excellent magnetoresponsive properties of MFNPs, numerous exciting *in vivo* biomedical applications are created. These include imaging for non-invasive diagnosis of diseases [12], treatment of diseases with hyperthermia [13], magnetically driven nanorobots [14], magnetic activation of ion channel for cell signaling [15], manipulation of cell's function and fate [16,17], *and so on*. Despite the good establishment of these concepts, there is a significant challenge in obtaining effective MFNPs that can achieve full functionality *via* the efficient conversion of the external energy of magnetic field. As such, due to their poor conversion ability, this greatly hinders their transition from bench to bed.

As MFNPs are delivered to their biological targets, MFNPs have the ability to induce different cell response for modulating biological systems by converting the external energy of the magnetic fields into biosensitive signals, such as mechanical forces, heating stimuli, and inducing local field. In such process, the performance is strongly dependent on the magnetic characteristics of these MFNPs mediators. Thus, to effectively transduce biochemical signals, it is highly crucial to engineer MFNPs with enhanced magnetic response. Numerous of research studies have indicated that

* Corresponding author.
E-mail address: fanhm@nwu.edu.cn (H. Fan).

https://doi.org/10.1016/j.mtadv.2020.100119

biological effects generated by various MFNPs may vary by orders of magnitude, which is highly dependent on their intrinsic magnetic properties [13,18]. For instance, one of the magnetic parameters of MFNPs is saturation magnetization (*Ms*), and it is closely related to thermal conversion efficiency. It has been reported that *Ms* of MFNPs can be optimized *via* precise control of their size [19], composition [13], structure [3], and morphology [20]. Besides modifying individual nanoparticle, designing the assembly of MFNPs is another approach to improve the performance, whereby higher *Ms* can be realized. As such, to enhance their response to magnetic field, various strategies have been developed to fabricate assemblies or clusters of MFNPs [21]. Even though the employment of MFNPs *in vivo* diagnosis and therapy is still in its infancy, these proposed strategies have greatly relieved the concerns of poor conversion efficiency of MFNPs for advanced biomedical applications.

In this review, we describe the strategies used in the engineering of MFNPs with enhanced magnetic response for these pioneering biomedical applications. We focus on the recent progress on magnetically triggered *in vivo* biomedical applications mediated by MFNPs (Fig. 1). We cover the magnetoresponsive mechanism and the critical magnetic parameters of MFNPs that can influence the application performance. Innovative biomedical applications using MFNPs mediator are also highlighted. Furthermore, we explore the perspectives and challenges of employing MFNPs in biomedical applications. The aim of this review is to provide a comprehensive and systematic review of these magnetically responsive MFNPs in biomedical applications when subjected to external magnetic field and to discuss the future directions of this field.

2. MFNPs-based magnetoresponsive effects for biomedical applications

2.1. Magnetic resonance imaging

MFNPs have been used as magnetic resonance imaging (MRI) contrast agents in clinical setting [22]. The enhancement in MRI signal is ascribed to the dipole-dipole interaction between MFNPs and surrounding water molecules, to shorten the relaxation time of the longitudinal (T_1) or transverse (T_2) of the nearby water protons. Relaxivity (r_1 or r_2) is used to evaluate the contrast ability of the MR contrast agent. Based on the theoretical considerations, it is generally known that relaxation enhancement of contrast agents follows inner- and outer-sphere mechanisms. The inner-sphere proton relaxation requires direct bonding of water molecules to paramagnetic ions. In contrast, outer-sphere proton relaxation is related to the dephasing of coherent proton spins [1]. Therefore, relaxivity of the contrast agent is the sum of inner-sphere and outer-sphere contributions [23–27]. For MFNPs, outer-sphere

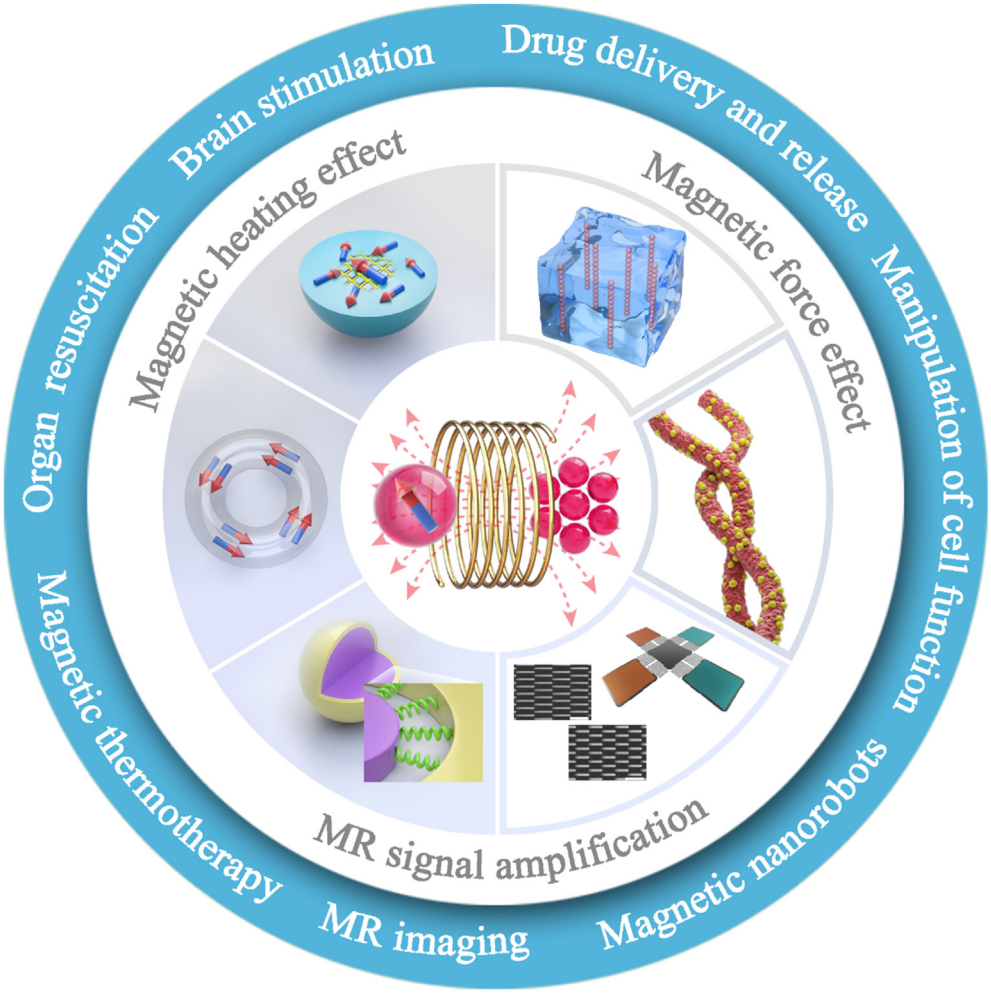

Fig. 1. Schematic illustration of engineered MFNPs with external magnetic actuation for various biomedical applications. MFNPs, magnetic ferrite nanoparticles.

contribution typically dominates the T_2 relaxation enhancement. However, when the size of the nanoparticle is smaller than 5 nm, contribution from inner-sphere mechanism cannot be neglected, which indicates that both outer-sphere and inner-sphere proton relaxation contributions are responsible for T_1 relaxation enhancement [25,28].

MFNPs exhibit a unique size-dependent magnetic property. For bulk magnetite, it possesses ferrimagnetic (FM) behavior, with multidomain magnetic structure. As the size of MFNPs decreases below a certain critical size, it becomes single domain within which the magnetic moments of free electrons are aligned parallel. It has shown that there exists a single domain limit formula which can determine the critical size of single domain for a spherical MFNP and is estimated to be $Dc \approx \frac{36\sqrt{AK}}{\mu_0 Ms^2}$ [29], where A is the exchange constant, K is the effective anisotropy constant that measures the energy per unit volume required to flip magnetization direction, μ_0 is the vacuum permeability, and Ms is the saturation magnetization. For different composition of MFNPs, the critical size will be different. With the further reduction in particle size, magnetization direction of MFNPs is randomized due to obvious thermal effects, which results in the observed superparamagnetic (SPM) behavior. As the particle size decreases to smaller than 5 nm, MFNPs become quasi-paramagnetic (QPM) due to the increase of the 'spin-canting effect'. It can be treated as a core/shell structure comprising a ferromagnetic core and paramagnetic shell (spin disorder layer). QPM IONPs are essentially SPM IONPs with an extremely low blocking temperature. Owing to the strong surface spin-canting effect, their magnetization curves at room temperature are more similar to paramagnetic characteristics. Traditional SPM IONPs show T_2 contrast effect, whereas QPM IONPs can be used as T_1 MRI contrast agent. However, as a result of their relatively poor relaxivities, their performances are still considered to be unsatisfactory. Gadolinium complexes are the most commonly used T_1 contrast agents in clinic. However, gadolinium complexes may release free gadolinium ions during metabolism, which have adverse side effects [30–33]. Engineering MFNPs have been used for many fascinating applications in the field of molecular imaging over the past decades. In the existing strategy, both r_1 and r_2 values can be controlled by modulating the composition [4,34,35], morphology [36,37], surface state [38], and assembly [39,40] of the NPs. In addition, engineering MFNPs can be used as a versatile platform for T_1-T_2 dual-modal contrast agents, and they can achieve T_1-T_2 switchable MRI (Fig. 2).

Generally, for MFNPs in motional averaging regime, the r_2 values increase as increasing the size. For example, Jun et al. reported that T_2-weighted MR signal intensity continuously increased as IONPs size increased from 4 nm to 12 nm [41]. While the size of MFNPs reaches a threshold, proton relaxation becomes governed by static dephasing regime, and its r_2 value reaches a limitation [42,43]. Lee et al. [4] further investigated the effect of doping on the T_2 contrast ability of artificially engineered IONPs. Because Mn^{2+} possessed 5 unpaired electrons, $MnFe_2O_4$ NPs exhibited the highest magnetic moment and r_2 relaxivity (358 $mM^{-1}s^{-1}$) as compared with other MFNPs under similar conditions. Zhao et al. [37] synthesized octapod IONPs with edge length of 30 nm, by introducing chloride anions. The as-synthesized octapod IONPs exhibited an ultrahigh r_2 value of 679.3 ± 30 $mM^{-1}s^{-1}$, hence revealing it as effective T_2 contrast agent for small tumor detection (Fig. 3A–B). This result was attributed to the larger effective radius of octapod IONPs as compared with that of spherical IONPs with equivalent solid volume. In addition, the same research group also reported $Zn_xFe_{3-x}O_4$ (x = 0.44) octapods which exhibited a remarkable r_2 value of 989.1 $mM^{-1}s^{-1}$ at 7.0 T, and it could sensitively detect metastatic hepatic tumors at low dose (one tenth of the regular dose) [44]. Liu et al. investigated the surface effect on the T_2 relaxivity of $MnFe_2O_4$ NPs [38]. As branch methoxy poly (ethylene glycol) (mPEG)-g-PEI polymers could hinder the diffusion of water molecules, the mPEG-g-PEI modified MFNPs possessed a remarkably high T_2 relaxivity of up to 331.8 $mM^{-1}s^{-1}$. Gao et al. [45] developed a tumor microenvironment responsive nanoprobe through a glutathione-triggered aggregation. In addition, by labeling Fe_3O_4 with ^{99m}Tc, the responsive particle probe could achieve sensitive single-photon emission computed tomography and MR dual-modality imaging of tumor *in vivo*.

When traditional SPM IONPs are used as MR T_2 contrast agents, their low-signal areas can be easily confused during clinical applications. To overcome the shortcomings of SPM IONPs-based T_2 contrast agents, the use of QPM IONPs as T_1 contrast agent has been successfully developed. Kim et al. synthesized monodispersed ultra-small IONPs for high-resolution blood pool imaging in rats [46]. Recently, the same research group reported the first study of the toxicity of ultra-small iron oxide nanoclusters in large animal models such as beagle dogs and macaques. It was then used as a MRI T_1 contrast agent for high-resolution angiography and diagnosis of cerebral ischemia in beagle dogs and macaques [2]. Zhang et al. [25] reported a general dynamic simultaneous thermal decomposition strategy for the controllable synthesis of monodispersed ultra-small MFNPs ($MnFe_2O_4$, $NiFe_2O_4$, and $CoFe_2O_4$). These ultra-small MFNPs were later demonstrated as multifunctional T_1 MR nanoprobe for *in vivo* high-resolution blood pool and liver-specific MRI simultaneously. In this case, metal doping could optimize water residence time (τ_m) to obtain a r_1 relaxivity of 8.43 $mM^{-1}s^{-1}$, which was about 1.8 times that of IONPs. By using ultra-small MFNPs as a good ultra-small magnetic ferrite nanocrystalline model system, this gave a clear relationship between chemical composition and T_1 MR signal enhancement effect. Moreover, ultra-small MFNPs-based active target MRI contrast agent were constructed by combining ultra-small MFNPs with tumor-targeting pentapeptide CREKA, which could detect ultra-small breast cancer metastases with high sensitivity [47]. By binding CREKA to the rich fibrin-fibronectin complex around the tumor microenvironment, these ultra-small MFNPs-CREKA could be recruited to the edge of the tumor metastasis and then Mn^{2+} was released in response to the tumor microenvironment. The local release of Mn^{2+} and its interaction with proteins led to the significant amplification of MRI T_1 signals. *In vivo* T_1 imaging results showed that this ultra-sensitive MRI T_1 probe could detect metastatic tumors with diameter as small as 0.39 mm, which greatly increased the detection limits of the previously reported MRI probes (Fig. 3C–E). Shen et al. [48] developed dotted core-shell NPs ($FeGd–HN_3–RGD_2$) with superhigh r_1 value and very low r_2/r_1 ratio for high-contrast T_1-weighted MRI of tumors. Macher et al. [49] prepared ultrathin iron oxide nanowhiskers to demonstrate the effect of the shape of IONPs on their MRI T_1 contrast effects. A strong paramagnetic signal was generated due to the high surface-to-volume ratio of the as-prepared ultrathin iron oxide nanowhiskers (2 nm × 20 nm), which indicated that the reported material could be considered as high-performing T_1 contrast agent. Zhou et al. [50] prepared Gd ions embedded iron oxide nanoplates (10 nm in length and 2 nm in thickness) with {100} facets exposed on the surface. Owing to the ultra-small size of Gd iron oxide nanoplates and the exposure of a large number of metal ions on the surface, the nanoplates showed excellent T_1 performance. More recently, Zeng et al. [23] showed that the binding affinity of anchoring ligands was strongly correlated to the magnetic moment of IONPs. In particular, higher binding affinity of the anchoring ligands could result in a lower magnetic moment of the resulted IONPs, whereby π-π and p-π conjugations between the anchoring ligands (*e.g.*, catechol and hydroxamate groups) and IONPs were

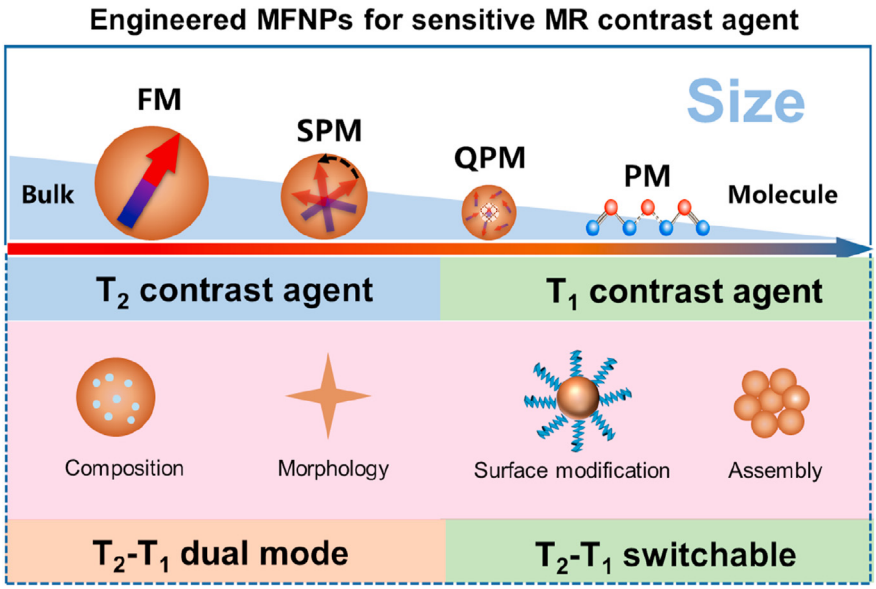

Fig. 2. Schematic illustration of the factors in engineering MFNPs to adjust their relaxivities. MFNPs, magnetic ferrite nanoparticles.

identified as the main reasons of enhancing the magnetization effect of IONPs.

To tailor the MRI contrast effect, engineered MFNPs can be used as T_1-T_2 dual-modal contrast agents or achieve T_1-T_2 switchable MRI. One method to design T_1-T_2 dual-mode contrast agent is *via* the combination of IONPs and Gd species in a 'core-shell' configuration. Choi et al. [51] demonstrated a concept of 'magnetically decoupled' core-shell design, whereby T_1 and T_2 signals could be modulated with the use of a separating layer. This strategy allowed the placement of T_2 contrast material at the core and the placement of T_1 contrast material at the shell. By inserting a non-magnetic separating layer (SiO_2) with tuneable thickness, T_1 and T_2 contrast effects could be modulated. Recently, the same research group reported a distance-dependent MR tuning sensing technology, in which the nanometer-scale separation distance between paramagnetic enhancer and a SPM quencher tuned the ON or OFF of the T_1 MRI signal. When the enhancer was separated from the quencher, T_1 MRI signal was ON. On the other hand, T_1 MRI signal was quenched as the enhancer came closer to the quencher. This MRI-based MRET could provide an alternative approach for investigating a variety of biological processes [52].

The doping strategy is used to develop T_1-T_2 dual-modal contrasts. Zhou et al. [53] embedded Gd species into SPM IONPs to achieve the synergistic enhancement of r_1 and r_2 relaxivities (Fig. 3F). Furthermore, the same research group reported that IONPs could be developed as T_1-T_2 dual-mode contrast agents by controlling the surface structures of different exposed facets of IONPs. Iron oxide nanoplates with Fe_3O_4 {111} facets showed T_1-T_2 dual-modal contrast abilities [54]. The enhancement in T_1 contrast was mainly due to the efficient chemical exchanges of the exposed Fe-rich surface of the nanoplate. On the other hand, the contribution of T_2 enhancement was dominated by the effective radius of the iron oxide nanoplate.

Controlled assembly of MFNPs can provide a unique approach to manipulate their collective magnetic properties. This in turn can directly influence their MR contrast effects, which is useful in improving the sensitivity of the imaging technique. Wang et al. [55] proved that the self-assembly strategy based on ultra-small IONPs (3.5 nm) could enhance the distribution of NPs in the tumor (Fig. 3G). In contrast to the large-size NPs, ultra-small IONPs could easily extravasate from blood vessels of tumor and penetrate into the tumor tissue. *In vivo* MRI revealed that ultra-small IONPs showed a 'bright' T_1 contrast signal when dispersed in the tumor vascular area, and it showed a 'dark' T_2 contrast signal in the tumor after 24 h. Lu et al. [39] constructed a pH-responsive ultra-small IONPs assembly using a special DNA i-motif. Under a normal physiological pH of 7.4, the probe retained its assembly configuration with an enhanced T_2-weighted effect. On the other hand, under an acidic pH of 5.5, the probe responsively disassembled into monodispersed NPs, with an enhanced T_1-weighted effect instead. This type of ultra-small IONPs assembly that responds to the tumor microenvironment could achieve accurate diagnosis of the small hepatocellular carcinomas. The same research group then designed a pH-sensitive IONPs assembly by cross-linking ultra-small IONPs with small-molecular aldehyde derivative ligands [56]. At neutral pH, the assembly was stable due to the formation of hydrazine linkages. However, when it was subjected to the tumor acidic microenvironment, T_1 signal appeared gradually, which resulted in the amplification of MR signal. Bai et al. reported an ultra-small IONPs-based MRI probe with a time-dependent T_1-T_2 contrast enhancement imaging effect [57]. After 30 min of intravenous injection, the probe showed the best T_1 enhancement effect in the tumor area. Over time, T_1 signal gradually disappeared, whereas T_2 contrast effect was gradually enhanced. This time-dependent contrast enhancement of T_1-T_2 could effectively improve the accuracy and sensitivity of MRI diagnosis. Recently, Li et al. [58] constructed a photosensitive ultra-small IONPs-based nanoprobe. This probe could adjust the assembly-disassembly of nanoclusters by switching the laser-irradiated switches, so as to realize the transformation of dynamic T_1-T_2 dual modes. As such, this can be used to enhance the dual-mode MRI of retention and targeted arthritis. Recently, Wang et al [59]. designed a unique two-way MR tuning T_1-T_2 nanoprobe that could increase the sensitivity and selectivity of MRI as compared with that in conventional techniques used in tumor detection. The paramagnetic Mn chelate (P—Mn) and a SPM IONPs were self-assembled to form a two-way MR tuning nanoprobe. T_1 and T_2 MRI signals were dually turned 'on' depending on the increased distance between Mn^{2+} and SPM IONPs, which was controlled by the integrity of the micelles. This strategy could enhance the sensitivity of MRI in the detection of

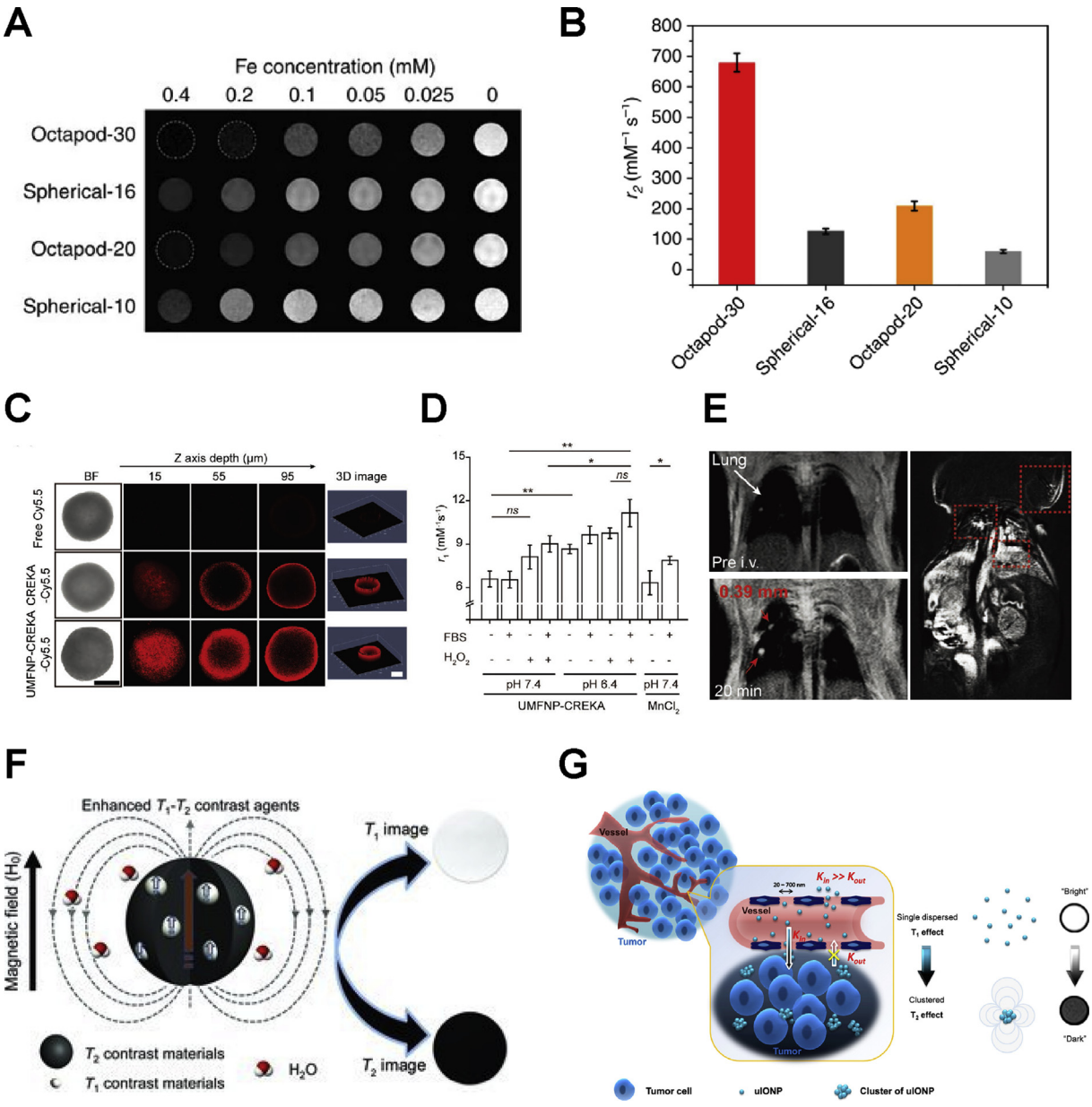

Fig. 3. (A–B) T_2-weighted images and r_2 values of octapod IONPs and spherical IONPs with same geometric volume. Adapted with permission [37]. Copyright 2013, Springer Nature. (C) Confocal microscopy images of 3D 4T1-Luc tumor spheroids after incubation with different materials. (D) r_1 values from T_1-weighted MR images of ultra-small MFNPs-CREKA. (E) T_1-weighted MRI detection of metastases in lung and spontaneous metastasis. Adapted with permission from a study by Li et al. [47]. Copyright 2019, John Wiley and Sons. (F) Schematic illustration of T_1-T_2 dual-modal contrast agents constructed by T_1 materials embedded into T_2 materials. Adapted with permission from a study by Zhou et al. [53]. Copyright 2012, John Wiley and Sons. (G) Ultra-small iron oxide assembly with T_1-T_2 MRI contrast switch can improve the distribution of NPs in tumor. Adapted with permission from a study by Wang et al. [55]. Copyright 2017, American Chemical Society. IONPs, iron oxide nanoparticles; MFNPs, magnetic ferrite nanoparticles.

early-stage small lesions, and it could also improve the accuracy of MRI-guided surgical procedures.

2.2. Magnetomechanical response in biomedical application

MFNPs can also transform the external energy of magnetic field into mechanical energy [60–62]. In a uniform magnetic field, MFNPs experience a torque τ that acts on the MFNPs to align the magnetic moment m with the field direction; $\tau = mB = \mu_0 VMH$, where, M represents the volumetric magnetization, V represents the volume of NP, and μ_0 represents the vacuum permeability. The magnitude of the magnetic force can be determined according to the following equation; $F = \nabla(m \cdot B)$, where, m and B represent the magnetic moment and magnetic field intensity, respectively. The magnitude and direction of magnetic force and torque are dependent on the size and intrinsic Ms of MFNPs, and the strength, gradient, and direction of the magnetic field [63]. Therefore, it is possible to optimize the magnetic properties of MFNPs by adjusting their physical parameters so as to fulfill the desired biomedical application.

2.2.1. Manipulation of cell function

In a magnetic field with a lower frequency, MFNPs tend to convert magnetic energy into mechanical energy, rather than thermal energy [60]. Various common low-frequency magnetic fields include static magnetic field, rotating magnetic field, and

pulsed magnetic field. MFNPs have ability to give traction stimulation to cells by static magnetic field. Wong et al. [64] have conducted in-depth research in this area. The basis of their research is to connect IONPs to the carrier and modify other molecules on the NPs to enable the cells to adhere to the particles and then gave the cells traction by the static magnetic field (Fig. 4A). These stimulations could regulate the proliferation, adhesion, migration, and differentiation of mesenchymal stem cells [16]. These also could manipulate the adhesion and polarization of macrophages [65], which could lead to good application effects *in vivo* (Fig. 4B). Rotating magnetic field is another kind of low-frequency magnetic field which is widely used. Under such magnetic field, the particles will produce torsional stimulation, which usually will cause damage to the cells, and even to the extent of killing the cells. Shen et al. [66] reported that under a rotating magnetic field of 15 Hz and 40 mT, IONPs firstly self-assembled into rods, and then it generated torsion (Fig. 4C). This led to the destruction of plasma membrane or mitochondria [67], which could precisely kill the cancer cells. Zhang et al. [68] also reported a method of destroying lysosomes through the rotation of particles to cause apoptosis. Pulsed magnetic fields have also been applied to IONPs to generate mechanical stimulation in recent years. Lunov et al. [69] used a magnetic field with a pulse interval of 15 μs and a magnetic field of up to 8 T to trigger the destruction of lysosomes by IONPs, which in turn led to apoptosis (Fig. 4D). Wong et al. [70] reported the use of 14 ± 10 Oe, 1–20 Hz biaxial pulsed magnetic field to achieve *in vitro* magnetic-induced apoptosis, by using IONPs with vortex magnetic domains. As low-frequency magnetic field exhibits safer field strength for the human body as compared with a higher-frequency magnetic field, the application of low-frequency magnetic field in biomedical field is particularly promising.

2.2.2. Drug delivery

Owing to its economical factor and operational simplicity, magnetic targeting system is widely investigated in the drug delivery application. For instance, Qiu et al. [71] demonstrated the increase in permeability of vascular endothelium by using magnetic force induced by IONPs to temporarily disrupt the endothelial adherent junctions. Therefore, this activated the paracellular transport pathway and facilitated the local extravasation of circulating substances, as well as ultimately enhancing the system dosing in certain parts of the transmission efficiency. Liu et al. [72] developed a magnetic platform composing of two oppositely polarized magnets that enabled the penetration of magnetic nanocarriers into the deep tumors. Using this method, they were able to demonstrate a 5-fold increase in the penetration depth and a 3-fold increase in the accumulation of MFNPs within the solid tumors (Fig. 5), when compared with enhanced permeability and retention. A biodegradable biohybrid helical shape magnetic robot, that was successfully fabricated from microalgae organism, was first reported by Yan et al [73]. Magnetic field was used to precisely control these robots in complex organisms so as to effectively carry and release drugs to the cancer cells. It was discovered that magnetic targeting could offer enhanced therapeutic efficacy, and it could improve the mice survival, when compared with passive targeting at drug doses of 5–8 mg of DTX/kg [74]. Thus, based on these successful reports, it is expected that magnetic targeting system can realize the efficient delivery of anticancer drugs, which plays an important role in effective tumor inhibition.

2.2.3. Magnetic robots

MFNPs can be assembled into nanorobots of different shapes, and they can later be magnetically driven to fulfill the diagnosis and

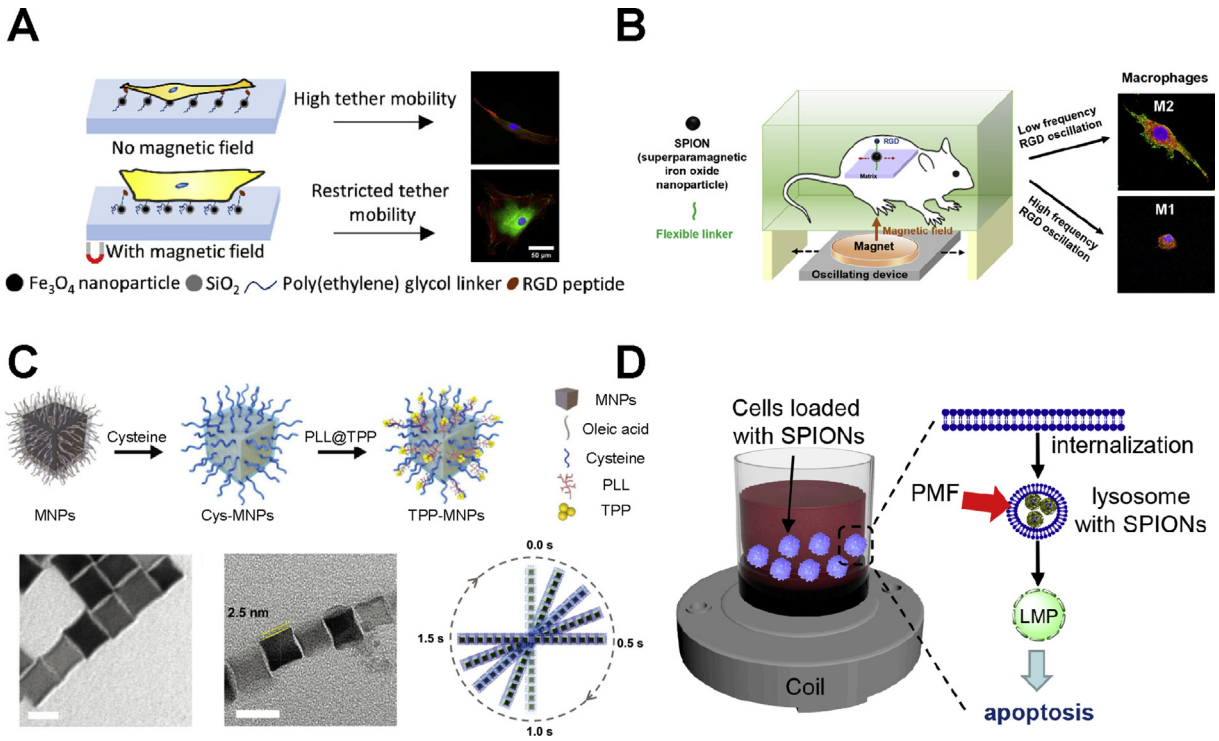

Fig. 4. (A) RGD-conjugated Fe_3O_4 on a planar substrate stretch MSCs in a static magnetic field. Adapted with permission from a study by Wong et al. [64]. Copyright 2017, American Chemical Society. (B) RGD-conjugated IONPs on a planar substrate control the polarization of macrophages in a static magnetic field *in vivo*. Adapted with permission from a study by Kang et al. [65]. Copyright 2017, American Chemical Society. (C) Modified IONPs self-assembled into a line and rotate in a rotation magnetic field. Adapted with permission from a study by Chen et al. [67]. Copyright 2019, John Wiley and Sons. (D) IONPs destroy lysosomes in pulsed magnetic field, which lead to cell apoptosis. Adapted with permission from a study by Lunov et al. [69]. Copyright 2019, MDPI. IONPs, iron oxide nanoparticles; MSCs, mesenchymal stem cells; RGD, Arg-Gly-Asp.

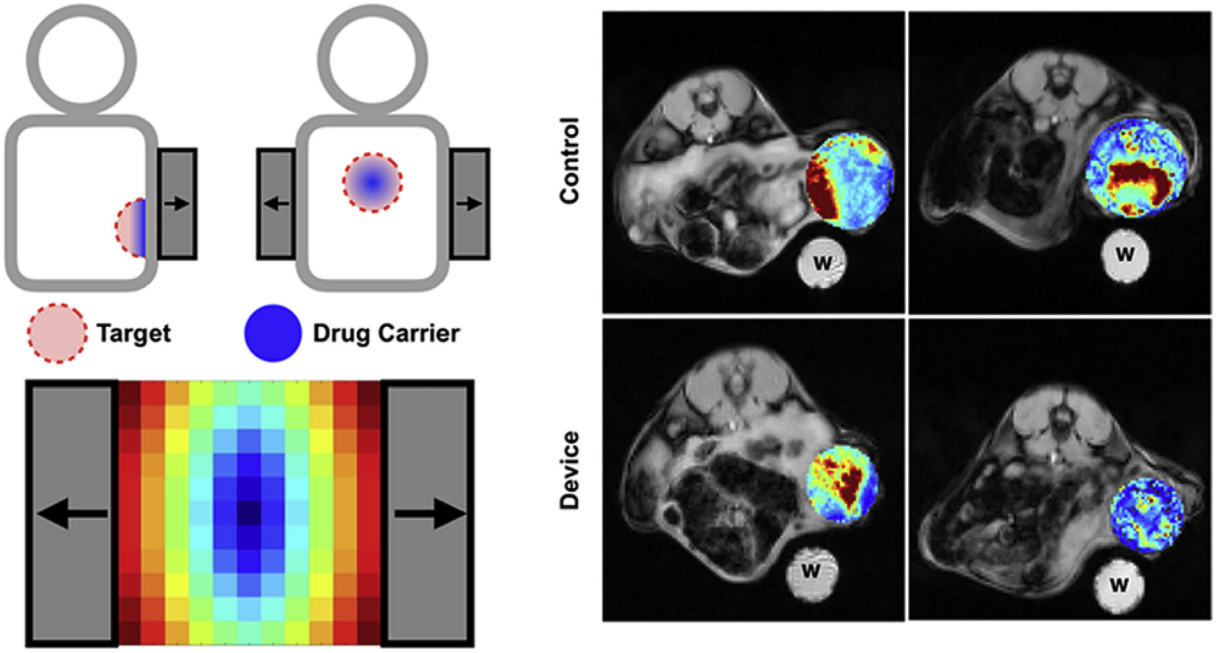

Fig. 5. Magnetic device, comprising two oppositely polarized magnets. This device enhances the magnetic drug targeting in deep tissues. Adapted with permission from a study by Liu et al. [72]. Copyright 2020, American Chemical Society.

treatment of diseases in complex biological environments [75,76]. For instance, Wu et al. [77] successfully achieved a controlled and efficient cluster movement in the vitreous body of the eye by developing a propeller-shaped nanorobot coated with a lubricating nanoliquid layer. Hu et al. [14] developed a rectangular-sheet-shaped magnetic soft robot composed of hard magnetic neodymium-iron-boron (NdFeB) microparticles embedded in silicone elastomer. By controlling the external magnetic field over time, this soft robot was able to change its shape to achieve various functions such as swimming, climbing, rolling, walking, jumping, and crawling. In addition, it could also accomplish functional tasks, such as grabbing an object and transporting it to a targeted location, and it was able to eject the cargo that was strapped onto the robot as well (Fig. 6A). Cui et al. [78] developed a strategy to program a single-domain nanomagnetic array on a flexible silicon nitride (Si_3N_4) substrate to encode multiple shape deformation instructions into a micromachine. This procedure was achieved by applying a specific magnetic field sequence to the nanomagnets with a suitably tailored switching field, which resulted in the specific shape transformations of the customized micromachines. Using this concept, they constructed a microscale 'bird' that was capable of performing complex behaviors such as, 'flapping', 'hovering', 'turning', and 'side-slipping' (Fig. 6B). Tang et al. [79] designed a DNA robot based on a super-soft and super-elastic magnetic DNA hydrogel. This DNA robot was able to exhibit shape-adaptive property, and it enabled magnetically driven navigational locomotion in confined and unstructured space (Fig. 6C–D). Magnetically driven nanorobots are expected to bring disruptive breakthroughs in the field of minimally invasive medicine in the future.

2.3. Magnetothermal response in biomedical application

MFNPs can convert electromagnetic energy into thermal energy when subjected to alternating magnetic field (AMF). The heat generation mechanism of MFNPs exposed to AMF is related to hysteresis or relaxation [80]. The heat generation in multidomain FM MFNPs is closely related to hysteresis dissipation [29]. For SPM MFNPs under AMF, magnetic loss is ascribed to Néel and Brown relaxation [80,81]. Néel relaxation refers to the internal thermal rotation of the magnetic moment of the particle within the crystal, which occurs when overcomes the anisotropy energy barrier $E_a=KV$ [82]. The Néel relaxation time is calculated by the following equation,

$$\tau_N = \tau_0 \exp\left(\frac{KV}{k_B T}\right) \quad (1)$$

where, τ_0 is the characteristic flipping frequency of 10^{-9} s, V the volume of nanoparticle, k_B the Boltzmann constant, T is the absolute temperature, and K is the anisotropy constant. Brown relaxation is due to the particle rotation in the solution under AMF. This rotation of MFNPs in solution generates rotational friction between the particles and the surrounding fluid, and thus resulting in heat production. Brown relaxation time is given by

$$\tau_B = \frac{3\eta V_H}{k_B T} \quad (2)$$

where, η is the viscosity of the solution, and V_H is the hydrodynamic volume of the NPs.

$$\tau_{eff} = \frac{\tau_N \tau_B}{\tau_{N+} \tau_B} \quad (3)$$

τ_{eff} is determined by τ_N and τ_B. MFNPs with smaller particle size are mainly affected by Néel relaxation, whereas Brown relaxation becomes prominent for larger particles [83]. The heating efficiency of MFNPs is generally evaluated by specific absorption rate (SAR) or intrinsic loss power (ILP) or specific loss power (SLP) [84–86].

$$SAR = \frac{\Delta T}{\Delta t} \frac{c}{m_{Fe}} \quad (4)$$

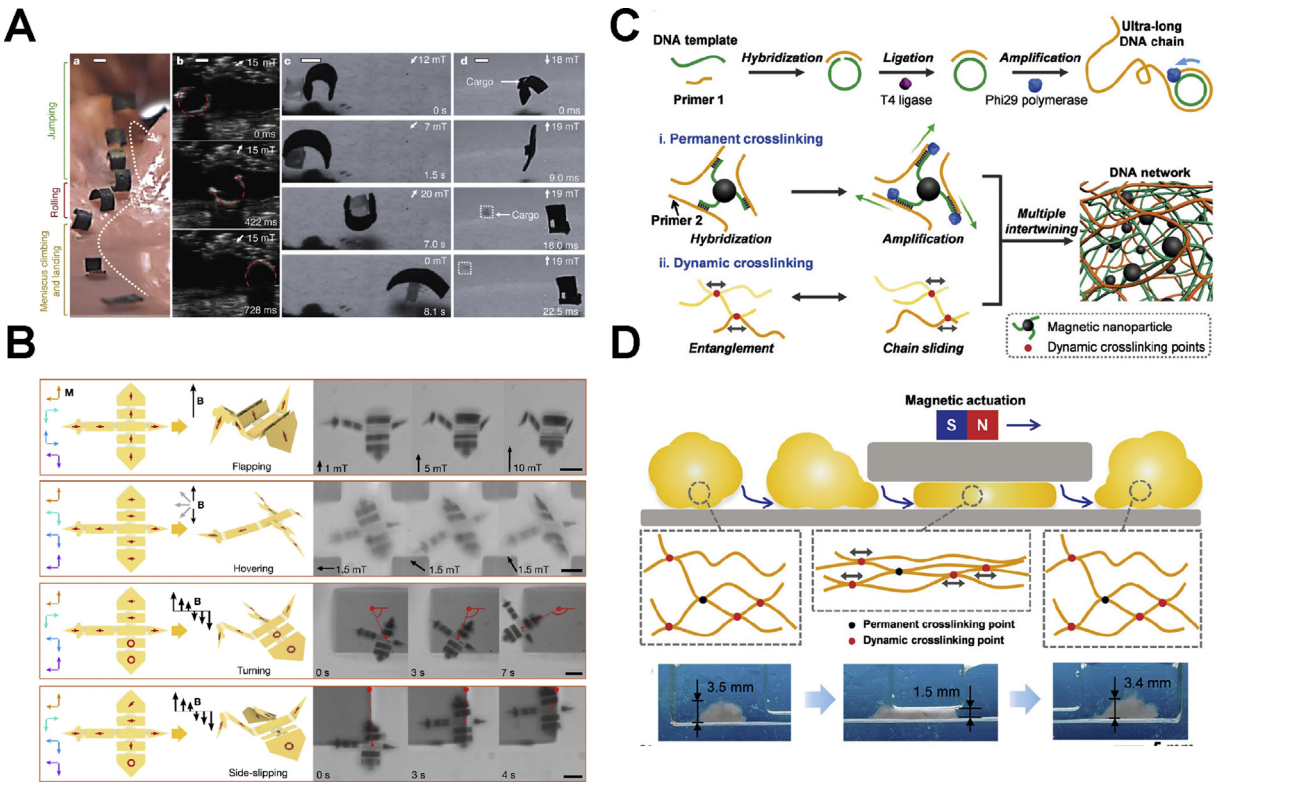

Fig. 6. (A) Small-scale soft-bodied robot in medical applications. Adapted with permission from a study by Hu et al. [14]. Copyright 2018, Springer Nature. (B) Schematic and optical images of a microscale 'bird' mimicking four flying modes. Adapted with permission from a study by Cui et al. [78]. Copyright 2019, Springer Nature. (C) Schematic of magnetic DNA hydrogel synthesis. (D) Shape adaptation characteristics of DNA robots. Adapted with permission from a study by Tang et al. [79]. Copyright 2019, John Wiley and Sons.

$$ILP = \frac{P}{\rho H^2 f} = \frac{SAR}{H^2 f} \tag{5}$$

where, c is the volumetric specific heat capacity of the solution, ρ is the density of MFNPs, m_{Fe} represents the mass concentration of magnetic element in the solution, and f and H are the frequency and strength of AMF, respectively.

$$SLP = \frac{\mu_0 \pi \chi''(f) H^2 f}{\rho \Phi} \tag{6}$$

where, Φ is the volume fraction of MFNPs, μ_0 and χ'' represent the vacuum permeability and imaginary component of the magnetic susceptibility, respectively. The major factor that needs to be considered to achieve high *SLP* is χ''.

$$\chi'' = \frac{\omega \tau_{eff}}{1 + \left(\omega \tau_{eff}\right)^2} \cdot \frac{\mu_0 M_S^2 V}{k_B T} \tag{7}$$

where, ω is the rotational angular frequency, τ_{eff} represents the effective relaxation time. Calorimetry is a straightforward way of measuring the amount of heat to determine SAR. Heating quantification is usually performed through the measurement of the temperature evolution of the sample. To estimate the SAR, the time-dependent temperature exponential curve was used, according to Equation (4), where $\frac{\Delta T}{\Delta t}$ is the initial slope of the time-dependent temperature curve [86–88]. Magnetic heating efficiency of MFNPs can be improved by adjusting the particle size, component, morphology, surface modification, and assembly to optimize the magnetic parameters.

2.3.1. Magnetic thermotherapy

Magnetic hyperthermia has recently attracted significant attention due to the noninvasive nature and no penetration limitation of magnetic field. Magnetic hyperthermia refers to the directional accumulation of MFNPs at the tumor site, and these NPs generate heat when being exposed to AMF to selectively kill the tumor cells [29,89]. Magnetic hyperthermia has been approved for clinical use in Europe, and clinical registration for prostate cancer treatment in the United States has completed [90].

Despite these advances, magnetic hyperthermia still suffers from some critical drawback. For instance, it requires the need for relatively large amounts of MFNPs due to the poor heating transfer efficiency of MFNPs (usually 1–2 M) [80]. A wide variety of strategies are proposed to optimize K, V, and M_S of MFNPs (Fig. 7), by modulating size, morphology, composition, surface modification, exchange-coupled and assembly, further to improve the heating efficiency of MFNPs. The SAR value increases as M_S increases, while reach a maximum value at a specific size [90,91]. The shape of MFNPs is another crucial factor in modulating the magnetic property, for optimizing the SAR value. The shape of the MFNPs can affect its surface atomic arrangement, which gives rise to the alteration in *Ms* and *K* [92]. It was reported that cubic MFNPs have larger SAR value than that of spherical MFNPs with an identical NPs volume, which resulted from the lower *K* and higher *Ms* for cubic MFNPs [20]. Liu et al. developed unique FM vortex-domain nanorings (FVIOs) with extremely high SAR up to 3050 W/g, an order of magnitude higher than that of the clinically used SPM IONPs. The significantly improved SAR value of FVIOs was related to the hysteresis loss arising from the vortex magnetic structure due to the shape anisotropy. It was shown in the *in vivo* study that the use of FVIOs could achieve efficient anti-tumor magnetic thermotherapy at low dose (0.3 mg/cm^3 of tumor tissue) (Fig. 8A–C) [93].

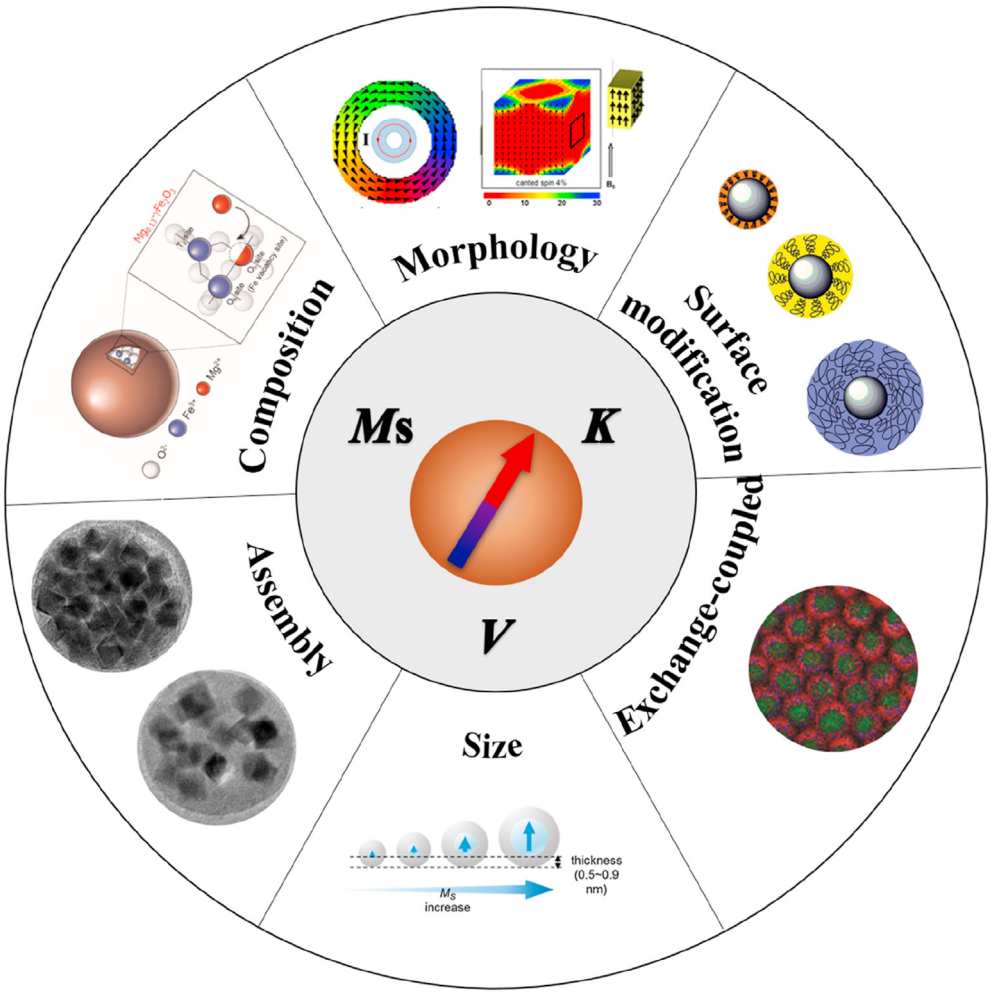

Fig. 7. The strategies toward engineering MFNPs with improved magnetic heating efficiency. Adapted with permission from a study from Noh et al. [80]. Copyright 2017, Elsevier. Adapted with permission from a study by Lee et al. [3]. Copyright 2011, Springer Nature. Adapted with permission from a study by Jang et al. [13]. Copyright 2017, John Wiley and Sons. Adapted with permission from a study by Noh et al. [20]. Copyright 2012, American Chemical Society. Adapted with permission from a study by Liu et al. [95]. Copyright 2012, Royal Society of Chemistry. Adapted with permission from a study by Liu et al. [96]. Copyright 2013, Royal Society of Chemistry.

The exchange-coupled MFNPs composed of magnetically hard and soft phases of the bio-magnetic material can improve the heating efficiency by optimizing the exchange anisotropy of MFNPs. Lee et al. [3] designed a series of exchange-coupled core-shell MFNPs, *i.e.*, $CoFe_2O_4$@$MnFe_2O_4$, $CoFe_2O_4$@Fe_3O_4, $MnFe_2O_4$@$CoFe_2O_4$, and Fe_3O_4@$CoFe_2O_4$, to tune the *K* and *Ms*, whereby a significant enhancement of SLP from 1000 to 4000 W/g was achieved. Composition modulation, for instance, divalent transition metal cations such as Fe^{2+}, Mg^{2+}, Mn^{2+}, Co^{2+}, Ni^{2+} or Zn^{2+} can be doped in the material, and it is shown that *K* and *Ms* of MFNPs can be adjusted to further improve its SAR [4,13,94]. Jang et al. [13] developed a biocompatible SPM magnesium-doped γ-Fe_2O_3 nanoparticle. By controlling the doping content of Mg^{2+} in γ-Fe_2O_3, the as-synthesized $Mg_{0.13}$@γ-Fe_2O_3 exhibited higher ILP (14 nHm^2kg^{-1}) as compared with commercial Fe_3O_4 (Feridex, ILP = 0.15 nHm^2kg^{-1}). $Mg_{0.13}$-γ-Fe_2O_3 possessed promising thermal effects that can kill the tumors completely, as indicated by the *in vivo* magnetic hyperthermia study. In addition, Liu et al. [95] prepared a series of different molecular weights phosphorylated mPEG coated MFNPs to study the influence of the surface of MFNPs on SAR. As the molecular weights of the coating polymer decreased from 5000 to 2000, a highest SAR value of 930 W/g was achieved for 19 nm Fe_3O_4 core. The assembly of MFNPs can also increase *Ms* significantly, thereby improving the heating efficiency. Albarqi et al. [21] reported a biocompatible magnetic nanocluster which composed of hexagon-shaped cobalt and manganese-doped IONPs, with enhanced heating efficiency.

Conventionally, magnetic thermotherapy is theoretically believed to be effective at temperature above 316 K, as MFNPs heaters can kill cancer cells only beyond this elevated temperature due to energy dissipation in AMF. In contrast, recent studies have shown that the magnetothermal effect mediated by MFNPs significantly enhance the generation of reactive oxygen species (ROS) in tumor microenvironment, thereby achieving efficient inhibition of solid tumors. Ma et al. [97] designed a biocompatible Fe_3O_4-Pd NPs which could simultaneously achieve significantly high magnetic photoheating efficiency and enhanced ROS generation. It was shown in the antitumor experiment that the tumor was completely eliminated on Day 18, and the inhibition rate toward 4T1 orthotopic breast tumors was 100% (Fig. 8D–G). Motivated by the positive result reported in the previous work, Liu et al. recently proposed a new type of magnetothermodynamic (MTD) therapy. This proposed MTD therapy addressed the limitations of traditional magnetic hyperthermia, and it combined magnetic heating of IONPs with its immune effect related to the induction of active oxygen so as to effectively inhibit tumor growth. In accordance with the results from the *in vitro* and *in vivo* experiments, it was indicative that the amplification of ROS

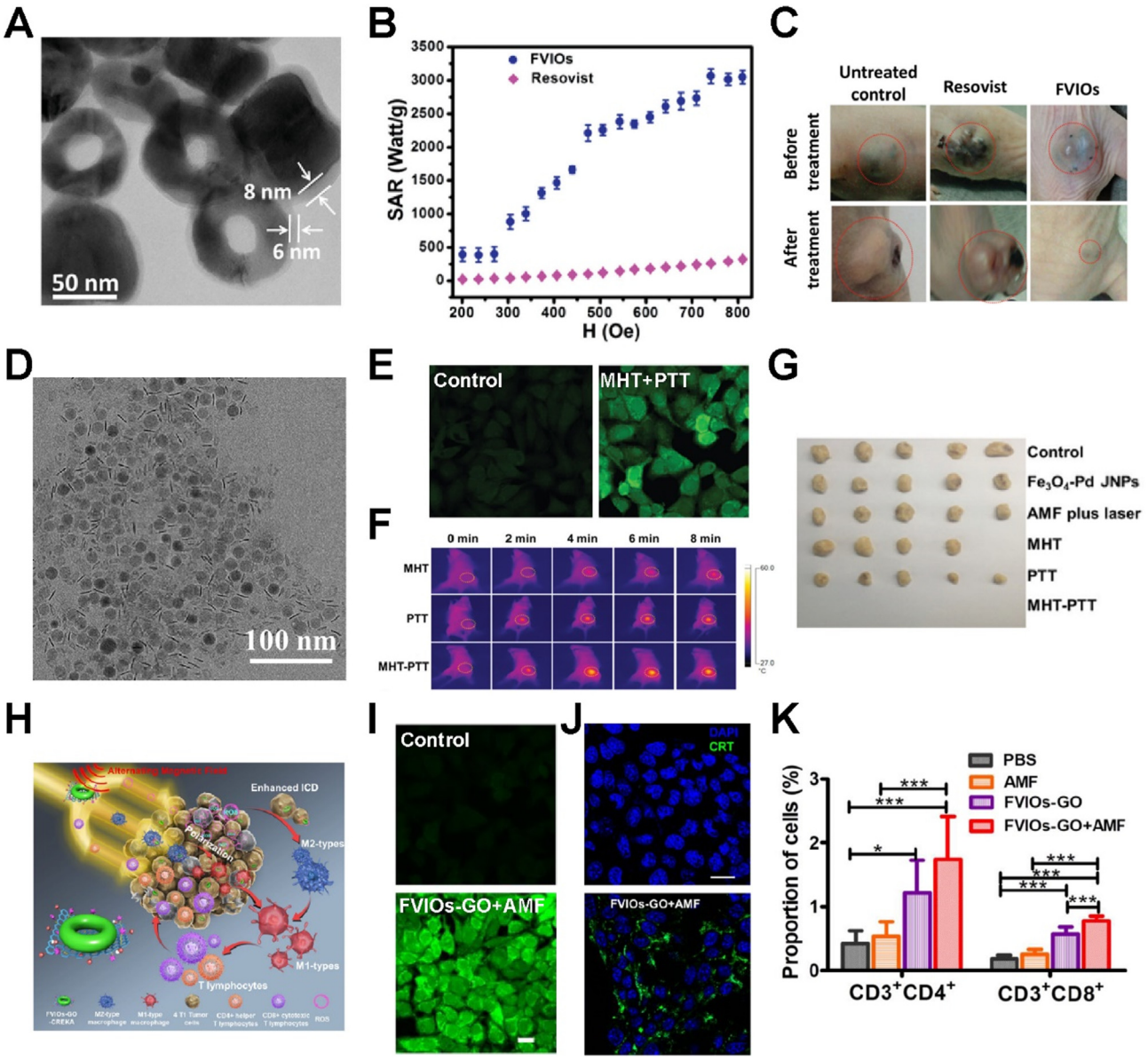

Fig. 8. (A) TEM image of FVIOs. (B) Comparison of SAR for FVIOs and Resovist in different fields. (C) Photographs of nude mice after treatment with untreated control, Resovist hyperthermia, and FVIOs hyperthermia, respectively. Adapted with permission from a study by Liu et al. [93]. Copyright 2015, John Wiley and Sons. (D) TEM image of Fe_3O_4-Pd NPs. (E) Confocal laser scanning microscope images of 4T1 cells after various treatments. Generation of ROS was monitored using DCFH-DA (green). (F) Thermal IR imaging of 4T1 tumor-bearing mice after intravenous injection of Fe_3O_4-Pd NPs exposed to AMF, 808 nm laser or AMF plus 808 nm laser. (G) Digital photos of tumor tissues excised from mice after subjected to different treatment. Adapted with permission from a study by Ma et al. [97]. Copyright 2019, Royal Society of Chemistry. (H) The proposed mechanism of FVIOs-GO mediated MTD by combination of heating effect and ROS related immunologic effect to efficiently eliminate the tumors at a physiological tolerated temperature. (I) Confocal laser scanning microscope images of 4T1 cells after various treatments. Generation of ROS was monitored using DCFH-DA (green). (J) Confocal laser scanning microscope images of CRT exposure in 4T1 cells after various treatment. (K) The percentages of $CD3^+CD4^+/CD3^+CD8^+$ T cell in the tumor tissue. Adapted with permission from a study by Liu et al. [98]. Copyright 2020, American Chemical Society. (For interpretation of the references to color in this figure legend, the reader is referred to the Web version of this article.) FVIOs, ferrimagnetic vortex-domain nanorings; CRT, calreticulin; SAR, specific absorption rate; ROS, reactive oxygen species; TEM, Transmission electron microscope.

generation was the main factor that induced immune response in the hypoxic tumor microenvironment, while keeping the physiological tolerance temperature below 313 K. This was supported by the 83% 4T1 breast cancer cell surface exposed calreticulin, macrophage polarized to proinflammatory M1 phenotype, and tumor-infiltrating T lymphocytes were further elevated (Fig. 8H–K) [98]. The proposition of MTD therapy has promoted the development of traditional magnetic hyperthermia, which significantly improves the antitumor effect, and it provides new concepts for precise and efficient magnetic thermotherapy in the future.

2.3.2. Drug release

MFNPs induce a thermal stimulus when subjected to AMF, and such thermal stimulus can also be used in controlling the release of chemotherapeutic drug [99,100]. Currently, various methods such as thermosensitive chemical bond breaking, and thermoresponsive molecular phase transition, *and so on* have been developed as means to control the drug release. For instance, Chen et al. [101] designed a stimuli-responsive nanoparticle platform (Mag@MSNs-AMA-CD) that could be triggered under AMF to release DOX. The DOX release could be regulated by modifying the thermoresponsive molecular containing aliphatic azo group. Through the *in vitro*

experiment, it was demonstrated that the amount of DOX released was correlated to the duration of AMF exposure (Fig. 9). Riedinger et al. [8] used thermolabile azo-molecules to link drugs or dyes to the IONPs, whereby these azo bonds could be cleaved upon heating to release the cargo. Katagiri et al. [102] designed a thermoresponsive liposomes composed of thermosensitive block copolymers, IONPs and phospholipids. These liposomes could work as an ON-OFF switchable drug release system that could be triggered by AMF. Chen et al. [103] prepared a magnetothermally responsive nanohybrid drug carrier with a phase transition temperature above 310 K in physiological conditions. Such drug carrier showed consistent release of doxorubicin on demand by exploiting the heat generated in the nanocubes under AMF. The possibility of associating controllable drug release with tumor targeting will increase the appeal of using MFNPs in clinical personalized medicine.

2.3.3. Organ resuscitation

Convective warming is the 'standard method' for heating small amounts of frozen biological tissue. However, as the volume of biological tissue increases, convective warming will not be sufficiently uniform throughout the system, which results in the destruction of cell structure due to the crystallization of water. To date, successful rewarming of tissues vitrified in VS55, can only be achieved by convective warming of small volumes in the range of 1 mL [104]. Successful rewarming requires both uniform and fast rates to reduce thermal mechanical stress and nucleation of cracks and also to prevent rewarming phase crystallization. To address such limitation, MFNPs that can generate heat rapidly and uniformly under AMF, can be used to improve the thawing process of cryopreserved biomaterials.

Manuchehrabadi et al. [105] reported the successful thawing of heart valves and blood vessels of large animals with a maximum preservation solution volume of 80 mL by coating silicon dioxide onto IONPs (Fig. 10A). Each part of the tissue could be uniformly heated at an approximately similar rate, without generating ice crystals. Once the tissue was completely melted, the NPs were washed away to obtain a relatively pure and active tissue. It was clearly demonstrated in the comparative test experiment at the cell

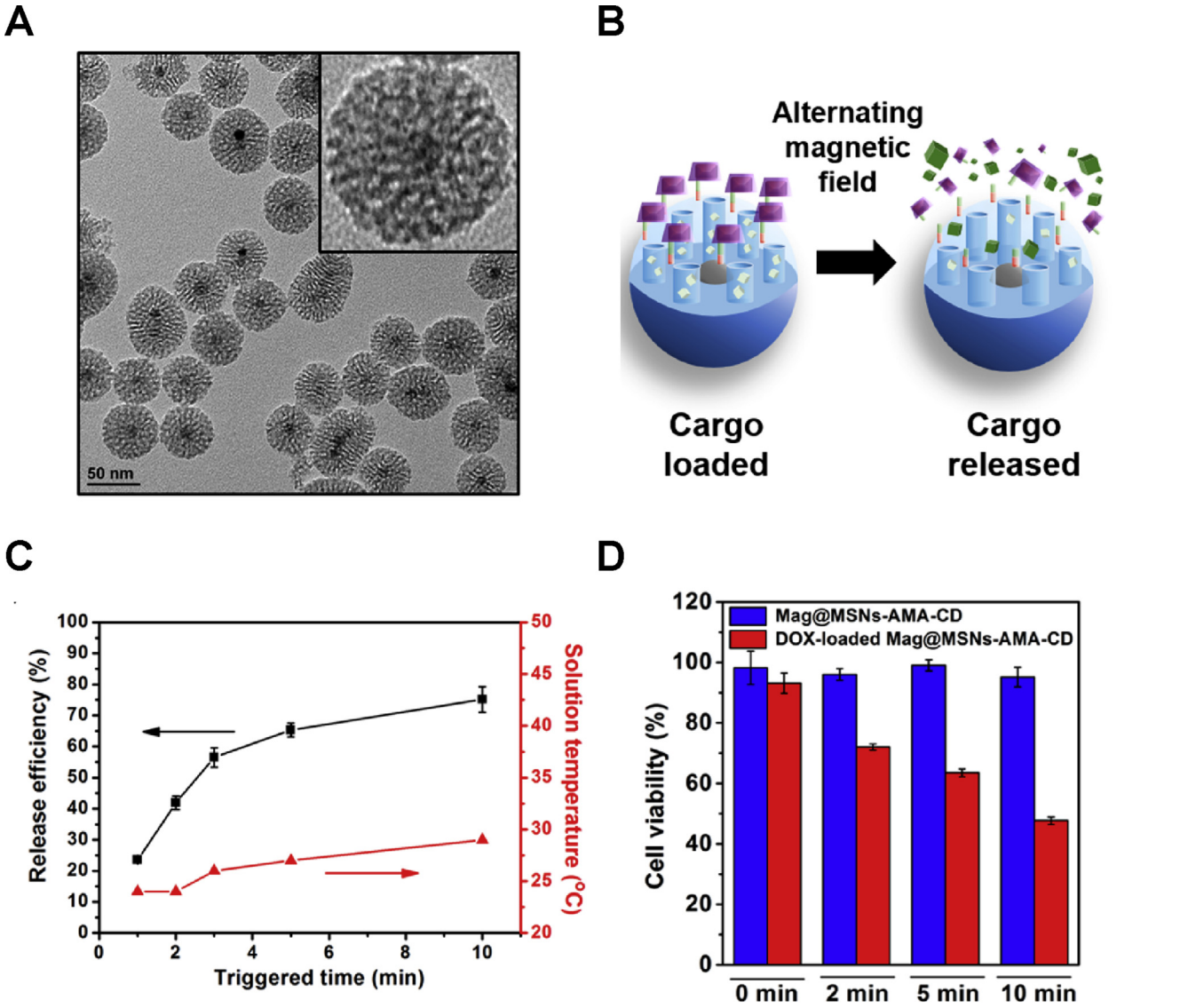

Fig. 9. (A) TEM image of Mag@MSNs-AMA. (B-D) The release of cargo by magnetic stimulation. Adapted with permission from a study by Chen et al. [101]. Copyright 2019, American Chemical Society. TEM, Transmission electron microscope.

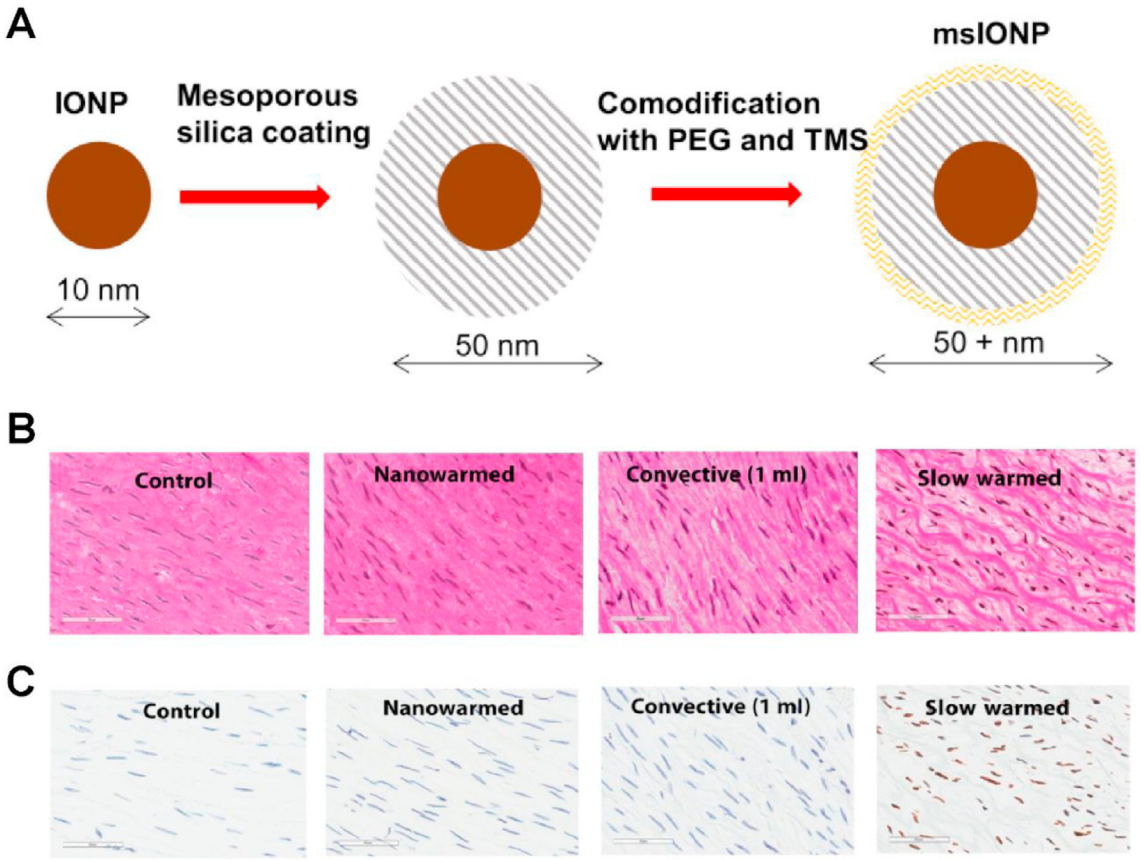

Fig. 10. (A) Schematic illustration detailing the synthesis of msIONPs. (B-C) H&E-stained and TUNEL-stained images in different treatment. Adapted with permission from a study by Manuchehrabadi et al.[105]. Copyright 2017, The American Association for the Advancement of Science. IONPs, iron oxide nanoparticles.

level that the tissue recovered *via* this nanoheating technology was basically similar as the normal tissue. This result indicated that such nanoheating technology did not cause damage to the tissue, whereas other tissues recovered *via* traditional heating methods exhibited different degrees of injury (Fig. 10B–C). As such, based on their report, the use of magnetic heating effects of MFNPs presents significant potential in the realization of cryopreservation of human organs.

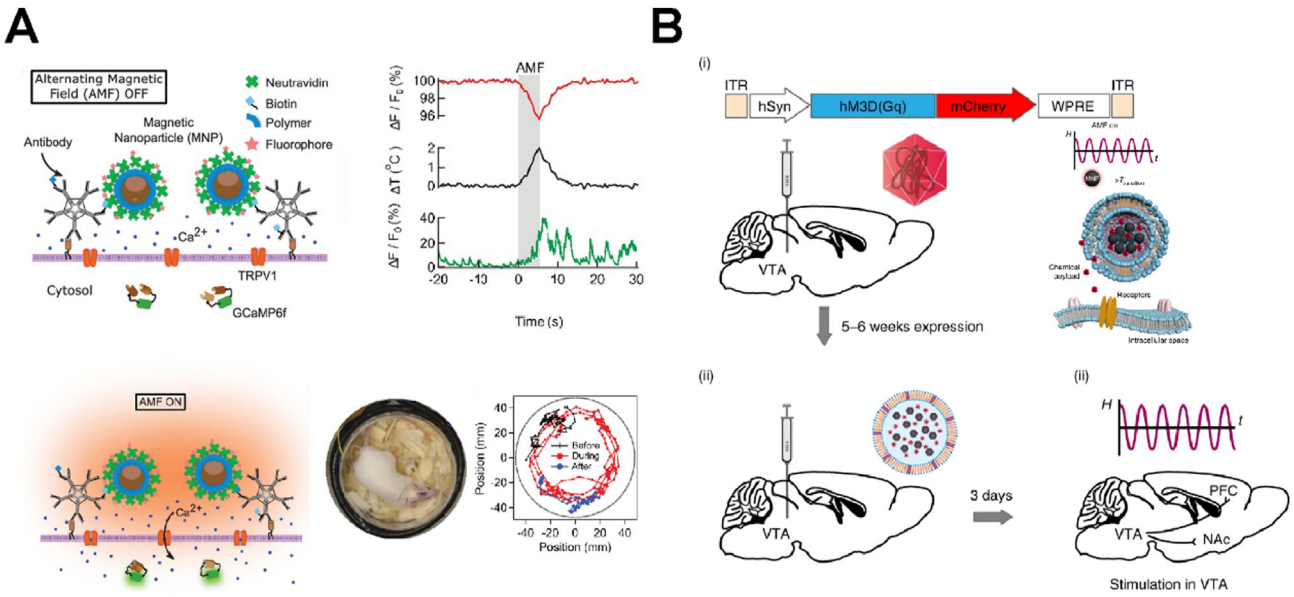

Fig. 11. (A) MFNPs under AMF activate TPRV1 channels. Adapted with permission from a study by Munshi et al. [112]. Copyright 2017, eLife Sciences Publications. (B) Chemomagnetic stimulation *in vivo*. Adapted with permission from a study by Rao et al. [113]. Copyright 2019, Springer Nature. AMF, alternating magnetic field; MFNPs, magnetic ferrite nanoparticles.

2.3.4. Brain stimulation

MFNPs can be used in brain stimulation based on the magnetothermal effect under AMF, and such method is known as the magneto-thermo-genetics method (magnetogenetics) [106,107]. Comparing with the conventional methods (electrodes and chemicals) and second-generation method (ultrasound and optogenetics), magnetogenetics has the advantages of cell type specificity, superior spatial and temporal resolution, as well as it does not require the tethering of the animals to an energy source. As such, there is an immense interest in using magnetogenetics to activate the heat-sensitive transient receptor potential vanilloid 1 (TRPV1, ˃316 K) to achieve further brain stimulation. SPM NPs, including $MnFe_2O_4$, Fe_3O_4, ferritin, Co-ferrite core@Mn-ferrite core-shell structure, have been used in the activation of thermosensitive TRPV1 channel. For example, it was first reported by Huang et al. [15] that $MnFe_2O_4$ NPs could be heated up to activate the TRPV1 channel. This resulted in an increase in intracellular calcium concentration, triggered action potentials in primary hippocampal neurons, and elicited retracting motions in partially anesthetized *C. elegans* worms. Fe_3O_4 NPs coated with anti-His antibody could target the TRPV1 channel with an extracellular His × 6 epitope tag, which could remotely activate TRPV1 and stimulate the synthesis and release of proinsulin for regulation of insulin production in mice [108]. They also synthesized a GFP-tagged ferritin nanoparticle intracellularly associated with a camelid anti-GFP-TRPV1, which could initiate calcium-dependent insulin transgene expression and modulate neuronal activities to induce feeding [109]. The same research group further developed a mutated chloride-permeable TRPV1, and achieved the neuronal inhibition *via* the same heat stimulation that responded to blood glucose levels and decreased feeding [110]. Chen et al. [111] demonstrated that Fe_3O_4 could remotely activate TRPV1 and evoke excitation in the targeted ventral tegmental area *in vivo*. Munshi et al. [112] successfully synthesized Co-ferrite@Mn-ferrite core-shell MFNPs with superior magnetothermal performances, which was used to stimulate neurocircuit and modulate behavior in awake mice, as shown in Fig. 11A. The heat dissipated by MFNPs could trigger the release of small-molecule (agonist or inhibitor) from the thermally sensitive lipid vesicles and be applied to chemogenetic activation of engineered receptors [113], as presented in Fig. 11B. The chemogenetic modulation of targeted neural circuits using MFNPs provides a vital and novel method for brain stimulation so as to investigate the brain functions and neurological diseases.

3. Conclusion and perspectives

In this review, we have summarized the magnetoresponsive properties of MFNPs that respond to an external magnetic field, the strategies of optimizing magnetic parameters of MFNPs to improve magnetothermal effects, magnetomechanical effects, and MRI signals. Furthermore, their respective magnetoresponsive biomedical applications reported in the recent years are also reviewed. Representative studies in each application have been summarized, which generally indicate the advantage of employing engineered MFNPs in enhancing the performance of existing applications (*e.g.* MR imaging, magnetic thermotherapy, drug delivery and release, *and so on*). It is shown that MFNPs is not only attractive in addressing the limitations of these existing applications, they can also be adopted in new exciting applications (*e.g.* brain stimulation, magnetic nanorobots, *and so on*), which can provide disruptive breakthroughs in the field of biomedicine. Despite the tremendous progress in biomedical application in the recent years, there is still a need to overcome several unresolved challenges:

1. Precise tailoring of MFNPs to the requirements of a specific application and further improvement in the application performance are necessary. The utmost important concern when employing MFNPs in human body is the safety aspect. In the clinical application, after achieving their diagnostic and therapeutic purposes, MFNPs should be eliminated by the living body without incurring any negative side effects. In the engineering of equipment and technology, it is also necessary to develop portable and controllable equipment that can generate magnetic field, and control system for basic research and clinical transformation.
2. The biological effects of magnetic fields should be studied in greater details, such as the multilevel biological effects of magnetic hyperthermia in tissue, cell, protein, and gene. Organism is considered to be a complex and constantly evolving ecosystem. When MFNPs enter into the organism, the delivery mechanism of these NPs to the biological targets should be worth considering.
3. MFNPs can be assembled into nanorobots of different shapes, and they can be magnetically driven to fulfill the diagnosis and treatment of diseases. They can also be used as drug delivery carriers in complex biological environments. The use of these magnetically driven, intelligent nanorobots in biomedical application is particularly exciting, which should capture increasing research interests in near future.

In principle, MFNPs mediated magnetic field is attractive due to its non-invasive nature and excellent penetration depth. More in-depth research work is needed to elucidate the potential of MFNPs in the future. As such, it is strongly believed that these interesting magnetoresponsive properties of MFNPs will be highly beneficial in the biomedical application in the future.

Declaration of competing interest

The authors declare that they have no known competing financial interests or personal relationships that could have appeared to influence the work reported in this article.

Acknowledgments

This work was supported by National Natural Science Foundation of China (Grant No. 81571809, 81771981, 82072063 and 61874088), National Natural Science Foundation for Young Scholars of China (Grant No. 31901003), Shaanxi Province Funds for Distinguished Young Scholars (Grant No. 202031900097), Natural Science Foundation of Shaanxi Province (Grant No. 2020JQ-610 and 2019JM-143), and China Postdoctoral Science Foundation (Grant No. 2018M641010, 2020M673631XBand 2019M653719).

References

[1] N. Lee, D. Yoo, D. Ling, M.H. Cho, T. Hyeon, J. Cheon, Iron oxide based nanoparticles for multimodal imaging and magnetoresponsive therapy, Chem. Rev. 115 (2015) 10637–10689.
[2] Y. Lu, Y. Xu, G. Zhang, D. Ling, M. Wang, Y. Zhou, Y. Wu, T. Wu, M.J. Hackett, B. Kim, H. Chang, J. Kim, X. Hu, L. Dong, N. Lee, F. Li, J. He, L. Zhang, H. Wen, B. Yang, S. Choi, T. Hyeon, D. Zou, Iron oxide nanoclusters for T_1 magnetic resonance imaging of non-human primates, Nat. Biomed. Eng. 1 (2017) 637–643.
[3] J.H. Lee, J.T. Jang, J.S. Choi, S.H. Moon, S.H. Noh, J.W. Kim, J.G. Kim, I.S. Kim, K.I. Park, J. Cheon, Exchange-coupled magnetic nanoparticles for efficient heat induction, Nat. Nanotechnol. 6 (2011) 418–422.
[4] J.H. Lee, Y.M. Huh, Y.W. Jun, J.W. Seo, J.T. Jang, H.T. Song, S. Kim, E.J. Cho, H.G. Yoon, J.S. Suh, J. Cheon, Artificially engineered magnetic nanoparticles for ultra-sensitive molecular imaging, Nat. Med. 13 (2007) 95–97.
[5] J. Gao, H. Gu, B. Xu, Multifunctional magnetic nanoparticles: design, synthesis, and biomedical applications, Acc. Chem. Res. 42 (2009) 1097–1107.

[6] K. Fan, C. Cao, Y. Pan, D. Lu, D. Yang, J. Feng, L. Song, M. Liang, X. Yan, Magnetoferritin nanoparticles for targeting and visualizing tumour tissues, Nat. Nanotechnol. 7 (2012) 459–464.

[7] O. Veiseh, J.W. Gunn, M. Zhang, Design and fabrication of magnetic nanoparticles for targeted drug delivery and imaging, Adv. Drug Deliv. Rev. 62 (2010) 284–304.

[8] A. Riedinger, P. Guardia, A. Curcio, M.A. Garcia, R. Cingolani, L. Manna, T. Pellegrino, Subnanometer local temperature probing and remotely controlled drug release based on azo-functionalized iron oxide nanoparticles, Nano Lett. 13 (2013) 2399–2406.

[9] V.S. Kalambur, B. Han, B.E. Hammer, T.W. Shield, J.C. Bischof, *In vitro* characterization of movement, heating and visualization of magnetic nanoparticles for biomedical applications, Nanotechnology 16 (2005) 1221–1233.

[10] S.B.R. Chang, J.L. Kirschvink, Magnetofossils, the magnetization of sediments, and the evolution of magnetite biomineralization, Annu. Rev. Earth Planet Sci. 17 (1989) 169–195.

[11] Y. Min, J.M. Caster, M.J. Eblan, A.Z. Wang, Clinical translation of nanomedicine, Chem. Rev. 115 (2015) 11147–11190.

[12] T.H. Shin, Y. Choi, S. Kim, J. Cheon, Recent advances in magnetic nanoparticle-based multi-modal imaging, Chem. Soc. Rev. 44 (2015) 4501–4516.

[13] J.T. Jang, J. Lee, J. Seon, E. Ju, M. Kim, Y.I. Kim, M.G. Kim, Y. Takemura, A.S. Arbab, K.W. Kang, K.H. Park, S.H. Paek, S. Bae, Giant magnetic heat induction of magnesium-doped gamma-Fe_2O_3 superparamagnetic nanoparticles for completely killing tumors, Adv. Mater. 30 (2018) 1704362.

[14] W. Hu, G.Z. Lum, M. Mastrangeli, M. Sitti, Small-scale soft-bodied robot with multimodal locomotion, Nature 554 (2018) 81–85.

[15] H. Huang, S. Delikanli, H. Zeng, D.M. Ferkey, A. Pralle, Remote control of ion channels and neurons through magnetic-field heating of nanoparticles, Nat. Nanotechnol. 5 (2010) 602–606.

[16] H. Kang, H.J. Jung, D.S.H. Wong, S.K. Kim, S. Lin, K.F. Chan, L. Zhang, G. Li, V.P. Dravid, L. Bian, Remote control of heterodimeric magnetic nanoswitch regulates the adhesion and differentiation of stem cells, J. Am. Chem. Soc. 140 (2018) 5909–5913.

[17] C. Wu, Y. Shen, M. Chen, K. Wang, Y. Li, Y. Cheng, Recent advances in magnetic-nanomaterial-based mechanotransduction for cell fate regulation, Adv. Mater. 30 (2018) 1705673.

[18] S. Tong, C.A. Quinto, L. Zhang, P. Mohindra, G. Bao, Size-dependent heating of magnetic iron oxide nanoparticles, ACS Nano 11 (2017) 6808–6816.

[19] Z. Nemati, J. Alonso, L.M. Martinez, H. Khurshid, E. Garaio, J.A. Garcia, M.H. Phan, H. Srikanth, Enhanced magnetic hyperthermia in iron oxide nano-octopods: size and anisotropy effects, J. Phys. Chem. C 120 (2016) 8370–8379.

[20] S.H. Noh, W. Na, J.T. Jang, J.H. Lee, E.J. Lee, S.H. Moon, Y. Lim, J.S. Shin, J. Cheon, Nanoscale magnetism control via surface and exchange anisotropy for optimized ferrimagnetic hysteresis, Nano Lett. 12 (2012) 3716–3721.

[21] H.A. Albarqi, L.H. Wong, C. Schumann, F.Y. Sabei, T. Korzun, X. Li, M.N. Hansen, P. Dhagat, A.S. Moses, O. Taratula, O. Taratula, Biocompatible nanoclusters with high heating efficiency for systemically delivered magnetic hyperthermia, ACS Nano 13 (2019) 6383–6395.

[22] N. Lee, T. Hyeon, Designed synthesis of uniformly sized iron oxide nanoparticles for efficient magnetic resonance imaging contrast agents, Chem. Soc. Rev. 41 (2012) 2575–2589.

[23] J. Zeng, L. Jing, Y. Hou, M. Jiao, R. Qiao, Q. Jia, C. Liu, F. Fang, H. Lei, M. Gao, Anchoring group effects of surface ligands on magnetic properties of Fe_3O_4 nanoparticles: towards high performance MRI contrast agents, Adv. Mater. 26 (2014) 2694–2698.

[24] R.B. Lauffer, Paramagnetic metal complexes as water proton relaxation agents for NMR imaging theory and design, Chem. Rev. 87 (1987) 901–927.

[25] H. Zhang, L. Li, X. Liu, J. Jiao, C.-T. Ng, J. Yi, Y. Luo, B.-H. Bay, L. Zhao, M. Peng, N. Gu, H. Fan, Ultrasmall ferrite nanoparticles synthesized via dynamic simultaneous thermal decomposition for high-performance and multifunctional T_1 magnetic resonance imaging contrast agent, ACS Nano 11 (2017) 3614–3631.

[26] D. Ni, W. Bu, E.B. Ehlerding, W. Cai, J. Shi, Engineering of inorganic nanoparticles as magnetic resonance imaging contrast agents, Chem. Soc. Rev. 46 (2017) 7438–7468.

[27] Z. Zhou, L. Yang, J. Gao, X. Chen, Structure-relaxivity relationships of magnetic nanoparticles for magnetic resonance imaging, Adv. Mater. 31 (2019), e1804567.

[28] Y. Miao, Q. Xie, H. Zhang, J. Cai, X. Liu, J. Jiao, S. Hu, A. Ghosal, Y. Yang, H. Fan, Composition-tunable ultrasmall manganese ferrite nanoparticles: insights into their *in vivo* T_1 contrast efficacy, Theranostics 9 (2019) 1764–1776.

[29] L. Wu, A. Mendoza-Garcia, Q. Li, S. Sun, Organic phase syntheses of magnetic nanoparticles and their applications, Chem. Rev. 116 (2016) 10473–10512.

[30] J.G. Penfield, R.F. Reilly Jr., What nephrologists need to know about gadolinium, Nat. Clin. Pract. Nephrol. 3 (2007) 654–668.

[31] T. Kanda, T. Fukusato, M. Matsuda, K. Toyoda, H. Oba, J. Kotoku, T. Haruyama, K. Kitajima, S. Furui, Gadolinium-based contrast agent accumulates in the brain even in subjects without severe renal dysfunction: evaluation of autopsy brain specimens with inductively coupled plasma mass spectroscopy, Radiology 276 (2015) 228–232.

[32] R.J. McDonald, J.S. McDonald, D.F. Kallmes, M.E. Jentoft, D.L. Murray, K.R. Thielen, E.E. Williamson, L.J. Eckel, Intracranial gadolinium deposition after contrast-enhanced MR imaging, Radiology 275 (2015) 772–782.

[33] R.J. McDonald, J.S. McDonald, D.F. Kallmes, M.E. Jentoft, M.A. Paolini, D.L. Murray, E.E. Williamson, L.J. Eckel, Gadolinium deposition in human brain tissues after contrast-enhanced MR imaging in ddult patients without intracranial abnormalities, Radiology 285 (2017) 546–554.

[34] Z. Zhou, L. Wang, X. Chi, J. Bao, L. Yang, W. Zhao, Z. Chen, X. Wang, X. Chen, J. Gao, Engineered iron-oxide-based nanoparticles as enhanced T_1 contrast agents for efficient tumor imaging, ACS Nano 7 (2013) 3287–3296.

[35] L. Yang, L. Ma, J. Xin, A. Li, C. Sun, R. Wei, B.W. Ren, Z. Chen, H. Lin, J. Gao, Composition tunable manganese ferrite nanoparticles for optimized T_2 contrast ability, Chem. Mater. 29 (2017) 3038–3047.

[36] Z. Zhou, X. Zhu, D. Wu, Q. Chen, D. Huang, C. Sun, J. Xin, K. Ni, J. Gao, Anisotropic shaped iron oxide nanostructures: controlled synthesis and proton relaxation shortening effects, Chem. Mater. 27 (2015) 3505–3515.

[37] Z. Zhao, Z. Zhou, J. Bao, Z. Wang, J. Hu, X. Chi, K. Ni, R. Wang, X. Chen, Z. Chen, J. Gao, Octapod iron oxide nanoparticles as high-performance T_2 contrast agents for magnetic resonance imaging, Nat. Commun. 4 (2013) 2266.

[38] X. Liu, Y. Wang, C. Ng, R. Wang, G. Jing, J. Yi, J. Yang, B. Bay, L.-Y.L. Yung, D. Fan, J. Ding, H. Fan, Coating engineering of $MnFe_2O_4$ nanoparticles with superhigh T_2 relaxivity and efficient cellular uptake for highly sensitive magnetic resonance imaging, Adv. Mater. Interfaces 1 (2014).

[39] J. Lu, J. Sun, F. Li, J. Wang, J. Liu, D. Kim, C. Fan, T. Hyeon, D. Ling, Highly sensitive diagnosis of small hepatocellular carcinoma using pH-responsive iron oxide nanocluster assemblies, J. Am. Chem. Soc. 140 (2018) 10071–10074.

[40] Z. Zhou, R. Tian, Z. Wang, Z. Yang, Y. Liu, G. Liu, R. Wang, J. Gao, J. Song, L. Nie, X. Chen, Artificial local magnetic field inhomogeneity enhances T_2 relaxivity, Nat. Commun. 8 (2017) 15468.

[41] Y.W. Jun, Y.M. Huh, J.S. Choi, J.H. Lee, H.T. Song, S. Kim, S. Yoon, K.S. Kim, J.S. Shin, J.S. Suh, J. Cheon, Nanoscale size effect of magnetic nanocrystals and their utilization for cancer diagnosis *via* magnetic resonance imaging, J. Am. Chem. Soc. 127 (2005) 5732–5733.

[42] D. Shigeoka, T. Yamazaki, T. Ishikawa, K. Miike, K. Fujiwara, T. Ide, A. Oshima, T. Hashimoto, D. Aihara, K. Kanda, A. Usui, Y. Hosokai, H. Saito, Y. Ichiyanagi, Functionalization and magnetic relaxation of ferrite nanoparticles for theranostics, IEEE Trans. Magn. 54 (2018) 6100707.

[43] A. Joos, N. Loewa, F. Wiekhorst, B. Gleich, A. Haase, Size-dependent MR relaxivities of magnetic nanoparticles, J. Magn. Magn Mater. 427 (2017) 122–126.

[44] L. Yang, C. Sun, H. Lin, X. Gong, T. Zhou, W.-T. Deng, Z. Chen, J. Gao, Sensitive contrast-enhanced magnetic reso42nance imaging of orthotopic and metastatic hepatic tumors by ultralow doses of zinc ferrite octapods, Chem. Mater. 31 (2019) 1381–1390.

[45] Z. Gao, Y. Hou, J. Zeng, L. Chen, C. Liu, W. Yang, M. Gao, Tumor microenvironment-triggered aggregation of antiphagocytosis ^{99m}Tc-labeled Fe_3O_4 nanoprobes for enhanced tumor imaging *in vivo*, Adv. Mater. 29 (2017) 1701095.

[46] B.H. Kim, N. Lee, H. Kim, K. An, Y.I. Park, Y. Choi, K. Shin, Y. Lee, S.G. Kwon, H.B. Na, J.G. Park, T.Y. Ahn, Y.W. Kim, W.K. Moon, S.H. Choi, T. Hyeon, Large-scale synthesis of uniform and extremely small-sized iron oxide nanoparticles for high-resolution T_1 magnetic resonance imaging contrast agents, J. Am. Chem. Soc. 133 (2011) 12624–12631.

[47] Y. Li, X. Zhao, X. Liu, K. Cheng, X. Han, Y. Zhang, H. Min, G. Liu, J. Xu, J. Shi, H. Qin, H. Fan, L. Ren, G. Nie, A bioinspired nanoprobe with multilevel responsive T_1-weighted MR signal-amplification illuminates ultrasmall metastases, Adv. Mater. 32 (2020) 1906799.

[48] Z. Shen, J. Song, Z. Zhou, B.C. Yung, M.A. Aronova, Y. Li, Y. Dai, W. Fan, Y. Liu, Z. Li, H. Ruan, R.D. Leapman, L. Lin, G. Niu, X. Chen, A. Wu, Dotted core-shell nanoparticles for T_1-weighted MRI of tumors, Adv. Mater. 30 (2018) 1803163.

[49] T. Macher, J. Totenhagen, J. Sherwood, Y. Qin, D. Gurler, M.S. Bolding, Y. Bao, Ultrathin iron oxide nanowhiskers as positive contrast agents for magnetic resonance imaging, Adv. Funct. Mater. 25 (2015) 490–494.

[50] Z. Zhou, C. Wu, H. Liu, X. Zhu, Z. Zhao, L. Wang, Y. Xu, H. Ai, J. Gao, Surface and interfacial engineering of iron oxide nanoplates for highly efficient magnetic resonance angiography, ACS Nano 9 (2015) 3012–3022.

[51] J.-S. Choi, J.-H. Lee, T.-H. Shin, H.-T. Song, E.Y. Kim, J. Cheon, Self-confirming "AND" logic nanoparticles for fault-free MRI, J. Am. Chem. Soc. 132 (2010) 11015–11017.

[52] J.S. Choi, S. Kim, D. Yoo, T.H. Shin, H. Kim, M.D. Gomes, S.H. Kim, A. Pines, J. Cheon, Distance-dependent magnetic resonance tuning as a versatile MRI sensing platform for biological targets, Nat. Mater. 16 (2017) 537–542.

[53] Z. Zhou, D. Huang, J. Bao, Q. Chen, G. Liu, Z. Chen, X. Chen, J. Gao, A synergistically enhanced T_1-T_2 dual-modal contrast agent, Adv. Mater. 24 (2012) 6223–6228.

[54] Z. Zhou, Z. Zhao, H. Zhang, Z. Wang, X. Chen, R. Wang, Z. Chen, J. Gao, Interplay between longitudinal and transverse contrasts in Fe_3O_4 nanoplates with (111) exposed surfaces, ACS Nano 8 (2014) 7976–7985.

[55] L. Wang, J. Huang, H. Chen, H. Wu, Y. Xu, Y. Li, H. Yi, Y.A. Wang, L. Yang, H. Mao, Exerting enhanced permeability and retention effect driven delivery by ultrafine iron oxide nanoparticles with T_1-T_2 switchable magnetic resonance imaging contrast, ACS Nano 11 (2017) 4582–4592.

[56] F. Li, Z. Liang, J. Liu, J. Sun, X. Hu, M. Zhao, J. Liu, R. Bai, D. Kim, X. Sun, T. Hyeon, D. Ling, Dynamically reversible iron oxide nanoparticle assemblies for targeted amplification of T_1-weighted magnetic resonance imaging of tumors, Nano Lett. 19 (2019) 4213–4220.

[57] C. Bai, Z. Jia, L. Song, W. Zhang, Y. Chen, F. Zang, M. Ma, N. Gu, Y. Zhang, Time-dependent T_1-T_2 switchable magnetic resonance imaging realized by c(RGDyK) modified ultrasmall Fe_3O_4 nanoprobes, Adv. Funct. Mater. 28 (2018) 1802281.
[58] X. Li, S. Lu, Z. Xiong, Y. Hu, D. Ma, W. Lou, C. Peng, M. Shen, X. Shi, Light-addressable nanoclusters of ultrasmall iron oxide nanoparticles for enhanced and dynamic magnetic resonance imaging of arthritis, Adv. Sci. 6 (2019) 1901800.
[59] Z. Wang, X. Xue, H. Lu, Y. He, Z. Lu, Z. Chen, Y. Yuan, N. Tang, C.A. Dreyer, L. Quigley, N. Curro, K.S. Lam, J.H. Walton, T.Y. Lin, A.Y. Louie, D.A. Gilbert, K. Liu, K.W. Ferrara, Y. Li, Two-way magnetic resonance tuning and enhanced subtraction imaging for non-invasive and quantitative biological imaging, Nat. Nanotechnol. 15 (2020) 482–490.
[60] Y.I. Golovin, S.L. Gribanovsky, D.Y. Golovin, A.O. Zhigachev, N.L. Klyachko, A.G. Majouga, M. Sokolsky, A.V. Kabanov, The dynamics of magnetic nanoparticles exposed to non-heating alternating magnetic field in biochemical applications: theoretical study, J. Nanopart. Res. 19 (2017) 59.
[61] J. Wu, P. Ning, R. Gao, Q. Feng, Y. Shen, Y. Zhang, Y. Li, C. Xu, Y. Qin, G.R. Plaza, Q. Bai, X. Fan, Z. Li, Y. Han, M.S. Lesniak, H. Fan, Y. Cheng, Programmable ROS-mediated cancer therapy via magneto-inductions, Adv. Sci. 7 (2020) 1902933.
[62] J. Kim, D. Seo, J. Lee, K.M. Southard, Y. Lim, D. Kim, Z.J. Gartner, Y.W. Jun, J. Cheon, Single-cell mechanogenetics using monovalent magnetoplasmonic nanoparticles, Nat. Protoc. 12 (2017) 1871–1889.
[63] Y.I. Golovin, S.L. Gribanovsky, D.Y. Golovin, N.L. Klyachko, A.G. Majouga, A.M. Master, M. Sokolsky, A.V. Kabanov, Towards nanomedicines of the future: remote magneto-mechanical actuation of nanomedicines by alternating magnetic fields, J. Contr. Release 219 (2015) 43–60.
[64] D.S. Wong, J. Li, X. Yan, B. Wang, R. Li, L. Zhang, L. Bian, Magnetically tuning tether mobility of integrin ligand regulates ddhesion, spreading, and differentiation of stem cells, Nano Lett. 17 (2017) 1685–1695.
[65] H. Kang, S. Kim, D.S.H. Wong, H.J. Jung, S. Lin, K. Zou, R. Li, G. Li, V.P. Dravid, L. Bian, Remote manipulation of ligand nano-oscillations regulates adhesion and polarization of macrophages *in vivo*, Nano Lett. 17 (2017) 6415–6427.
[66] Y. Shen, C. Wu, T.Q.P. Uyeda, G.R. Plaza, B. Liu, Y. Han, M.S. Lesniak, Y. Cheng, Elongated nanoparticle aggregates in cancer cells for mechanical destruction with low frequency rotating magnetic field, Theranostics 7 (2017) 1735–1748.
[67] M. Chen, J. Wu, P. Ning, J. Wang, Z. Ma, L. Huang, G.R. Plaza, Y. Shen, C. Xu, Y. Han, M.S. Lesniak, Z. Liu, Y. Cheng, Remote control of mechanical forces via mitochondrial-targeted magnetic nanospinners for efficient cancer treatment, Small 16 (2020), e1905424.
[68] E. Zhang, M.F. Kircher, M. Koch, L. Eliasson, S.N. Goldberg, E. Renstrom, Dynamic magnetic fields remote-control apoptosis via nanoparticle rotation, ACS Nano 8 (2014) 3192–3201.
[69] O. Lunov, M. Uzhytchak, B. Smolkova, M. Lunova, M. Jirsa, N.M. Dempsey, A.L. Dias, M. Bonfim, M. Hof, P. Jurkiewicz, Y. Petrenko, S. Kubinova, A. Dejneka, Remote actuation of apoptosis in liver cancer cells *via* magneto-mechanical Modulation of iron oxide nanoparticles, Cancers 11 (2019) 1873.
[70] W. Wong, W.L. Gan, N. Liu, W.S. Lew, Magneto-actuated cell apoptosis by biaxial pulsed magnetic field, Sci. Rep. 7 (2017) 10919.
[71] Y. Qiu, S. Tong, L. Zhang, Y. Sakurai, D.R. Myers, L. Hong, W.A. Lam, G. Bao, Magnetic forces enable controlled drug delivery by disrupting endothelial cell-cell junctions, Nat. Commun. 8 (2017) 15594.
[72] J.F. Liu, Z. Lan, C. Ferrari, J.M. Stein, E. Higbee-Dempsey, L. Yan, A. Amirshaghaghi, Z. Cheng, D. Issadore, A. Tsourkas, Use of oppositely polarized external magnets toimprove the accumulation and penetration of magnetic nanocarriers into solid tumors, ACS Nano 14 (2020) 142–152.
[73] X. Yan, Q. Zhou, M. Vincent, Y. Deng, J. Yu, J. Xu, T. Xu, T. Tang, L. Bian, Y.-X.J. Wang, K. Kostarelos, L. Zhang, Multifunctional biohybrid magnetite microrobots for imaging-guided therapy, Sci. Robot. 2 (2017). UNSP eaaq1155.
[74] K.T. Al-Jamal, J. Bai, J.T. Wang, A. Protti, P. Southern, L. Bogart, H. Heidari, X. Li, A. Cakebread, D. Asker, W.T. Al-Jamal, A. Shah, S. Bals, J. Sosabowski, Q.A. Pankhurst, Magnetic drug targeting: preclinical *in vivo* studies, mathematical modeling, and extrapolation to humans, Nano Lett. 16 (2016) 5652–5660.
[75] G.Z. Lum, Z. Ye, X. Dong, H. Marvi, O. Erin, W. Hu, M. Sitti, Shape-programmable magnetic soft matter, P. Natl. Acad. Sci. USA 113 (2016) E6007–E6015.
[76] J. Li, B. Ávila, W. Gao, L. Zhang, J. Wang, Micronanorobots for biomedicine delivery, surgery, sensing, and detoxification, Sci. Robot. 2 (2017), eaam6431.
[77] Z. Wu, J. Troll, H.-H. Jeong, Q. Wei, M. Stang, F. Ziemssen, Z. Wang, M. Dong, S. Schnichels, T. Qiu, P. Fischer, A swarm of slippery micropropellers penetrates the vitreous body of the eye, Sci. Adv. 4 (2018), eaat4388.
[78] J. Cui, T.Y. Huang, Z. Luo, P. Testa, H. Gu, X.Z. Chen, B.J. Nelson, L.J. Heyderman, Nanomagnetic encoding of shape-morphing micromachines, Nature 575 (2019) 164–168.
[79] J. Tang, C. Yao, Z. Gu, S. Jung, D. Luo, D. Yang, Super-soft and super-elastic DNA robot with magnetically driven navigational locomotion for cell delivery in confined space, Angew. Chem. Int. Ed. Engl. 59 (2020) 2490–2495.
[80] S.-h. Noh, S.H. Moon, T.-H. Shin, Y. Lim, J. Cheon, Recent advances of magneto-thermal capabilities of nanoparticles: from design principles to biomedical applications, Nano Today 13 (2017) 61–76.
[81] J. Mohapatra, M. Xing, J.P. Liu, Inductive thermal effect of ferrite magnetic nanoparticles, Materials 12 (2019) 3208.
[82] J.-P. Fortin, C. Wilhelm, J. Servais, C. Menager, J.-C. Bacri, F. Gazeau, Size-sorted anionic iron oxide nanomagnets as colloidal mediators for magnetic hyperthermia, J. Am. Chem. Soc. 129 (2007) 2628–2635.
[83] Q.A. Pankhurst, J. Connolly, S.K. Jones, J. Dobson, Applications of magnetic nanoparticles in biomedicine, J. Phys. D Appl. Phys. 36 (2003) R167–R181.
[84] M. Kallumadil, M. Tada, T. Nakagawa, M. Abe, P. Southern, Q.A. Pankhurst, Suitability of commercial colloids for magnetic hyperthermia, J. Magn. Magn Mater. 321 (2009) 1509–1513.
[85] B. Kozissnik, A.C. Bohorquez, J. Dobson, C. Rinaldi, Magnetic fluid hyperthermia: advances, challenges, and opportunity, Int. J. Hyperther. 29 (2013) 706–714.
[86] X. Liu, Y. Zhang, Y. Wang, W. Zhu, G. Li, X. Ma, Y. Zhang, S. Chen, S. Tiwari, K. Shi, S. Zhang, H.M. Fan, Y.X. Zhao, X.J. Liang, Comprehensive understanding of magnetic hyperthermia for improving antitumor therapeutic efficacy, Theranostics 10 (2020) 3793–3815.
[87] M. Coisson, G. Barrera, C. Appino, F. Celegato, L. Martino, A.P. Safronov, G.V. Kurlyandskaya, P. Tiberto, Specific loss power measurements by calorimetric and thermal methods on gamma-Fe_2O_3 nanoparticles for magnetic hyperthermia, J. Magn. Magn Mater. 473 (2019) 403–409.
[88] I. Andreu, E. Natividad, Accuracy of available methods for quantifying the heat power generation of nanoparticles for magnetic hyperthermia, Int. J. Hyperther. 29 (2013) 739–751.
[89] H. Zhang, X. Liu, Y. Zhang, F. Gao, G. Li, Y. He, M. Peng, H. Fan, Magnetic nanoparticles based cancer therapy: current status and applications, Sci. China Life Sci. 61 (2018) 400–414.
[90] M. Johannsen, U. Gneveckow, K. Taymoorian, B. Thiesen, N. Waldofner, R. Scholz, K. Jung, A. Jordan, P. Wust, S.A. Loening, Morbidity and quality of life during thermotherapy using magnetic nanoparticles in locally recurrent prostate cancer: results of a prospective phase I trial, Int. J. Hyperther. 23 (2007) 315–323.
[91] R. Rosensweig, Heating magnetic fluid with alternating magnetic field, J. Magn. Magn Mater. 252 (2002) 370–374.
[92] I. Castellanos-Rubio, I. Rodrigo, R. Munshi, O. Arriortua, J.S. Garitaonandia, A. Martinez-Amesti, F. Plazaola, I. Orue, A. Pralle, M. Insausti, Outstanding heat loss via nano-octahedra above 20 nm in size: from wustite-rich nanoparticles to magnetite single-crystals, Nanoscale 11 (2019) 16635–16649.
[93] X. Liu, Y. Yang, C.T. Ng, L. Zhao, Y. Zhang, B.H. Bay, H. Fan, J. Ding, Magnetic vortex nanorings: a new class of hyperthermia agent for highly efficient *in vivo* regression of tumors, Adv. Mater. 27 (2015) 1939–1944.
[94] J.T. Jang, H. Nah, J.H. Lee, S.H. Moon, M.G. Kim, J. Cheon, Critical enhancements of MRI contrast and hyperthermic effects by dopant-controlled magnetic nanoparticles, Angew. Chem. Int. Ed. Engl. 48 (2009) 1234–1238.
[95] X. Liu, H. Fan, J. Yi, Y. Yang, E.S.G. Choo, J. Xue, D. Fan, J. Ding, Optimization of surface coating on Fe_3O_4 nanoparticles for high performance magnetic hyperthermia agents, J. Mater. Chem. 22 (2012) 8235–8244.
[96] X. Liu, E.S.G. Choo, A.S. Ahmed, L. Zhao, Y. Yang, R.V. Ramanujan, J. Xue, D. Fan, H. Fan, J. Ding, Magnetic nanoparticle-loaded polymer nanospheres as magnetic hyperthermia agents, J. Mater. Chem. B 2 (2014) 120–128.
[97] X. Ma, Y. Wang, X. Liu, H. Ma, G. Li, Y. Li, F. Gao, M. Peng, H. Fan, X.-J. Liang, Fe_3O_4-Pd Janus nanoparticles with amplified dual-mode hyperthermia and enhanced ROS generation for breast cancer treatment, Nanoscale Horiz 4 (2019) 1450–1459.
[98] X. Liu, B. Yan, Y. Li, X. Ma, W. Jiao, K. Shi, T. Zhang, S. Chen, Y. He, X.J. Liang, H. Fan, Graphene oxide-grafted magnetic nanorings mediated magneto-thermodynamic therapy favoring reactive oxygen species-related immune response for enhanced antitumor efficacy, ACS Nano 14 (2020) 1936–1950.
[99] F. Assa, H. Jafarizadeh-Malmiri, H. Ajamein, H. Vaghari, N. Anarjan, O. Ahmadi, A. Berenjian, Chitosan magnetic nanoparticles for drug delivery systems, Crit. Rev. Biotechnol. 37 (2017) 492–509.
[100] C.S.S.R. Kumar, F. Mohammad, Magnetic nanomaterials for hyperthermia-based therapy and controlled drug delivery, Adv. Drug Deliv. Rev. 63 (2011) 789–808.
[101] W. Chen, C.A. Cheng, J.I. Zink, Spatial, temporal, and dose control of drug delivery using noninvasive magnetic stimulation, ACS Nano 13 (2019) 1292–1308.
[102] K. Katagiri, Y. Imai, K. Koumoto, T. Kaiden, K. Kono, S. Aoshima, Magneto-responsive on-demand release of hybrid liposomes formed from Fe_3O_4 nanoparticles and thermosensitive block copolymers, Small 7 (2011) 1683–1689.
[103] H. Kakwere, M.P. Leal, M.E. Materia, A. Curcio, P. Guardia, D. Niculaes, R. Marotta, A. Falqui, T. Pellegrino, Functionalization of strongly interacting magnetic nanocubes with (thermo)responsive coating and their application in hyperthermia and heat-triggered drug delivery, ACS Appl. Mater. Interfaces 7 (2015) 10132–10145.
[104] M.L. Etheridge, Y. Xu, L. Rott, J. Choi, B. Glasmacher, J.C. Bischof, RF heating of magnetic nanoparticles improves the thawing of cryopreserved biomaterials, Technology 2 (2014) 229–242.
[105] N. Manuchehrabadi, Z. Gao, J. Zhang, H. Ring, Q. Shao, F. Liu, M. McDermott, A. Fok, Y. Rabin, K. Brockbank, M. Garwood, C. Haynes, J. Bischof, Improved tissue cryopreservation using inductive heating of magnetic nanoparticles, Sci. Transl. Med. 9 (2017) 4586.
[106] S. Nimpf, D.A. Keays, Is magnetogenetics the new optogenetics? EMBO J. 36 (2017) 1643–1646.

[107] A. Tay, D. Di Carlo, Remote neural stimulation using magnetic nanoparticles, Curr. Med. Chem. 24 (2017) 537–548.
[108] S.A. Stanley, J.E. Gagner, S. Damanpour, M. Yoshida, J.S. Dordick, J.M. Friedman, Radio-wave heating of iron oxide nanoparticles can regulate plasma glucose in mice, Science 336 (2012) 604–608.
[109] S.A. Stanley, J. Sauer, R.S. Kane, J.S. Dordick, J.M. Friedman, Remote regulation of glucose homeostasis in mice using genetically encoded nanoparticles, Nat. Med. 21 (2015) 92–98.
[110] S.A. Stanley, L. Kelly, K.N. Latcha, S.F. Schmidt, X. Yu, A.R. Nectow, J. Sauer, J.P. Dyke, J.S. Dordick, J.M. Friedman, Bidirectional electromagnetic control of the hypothalamus regulates feeding and metabolism, Nature 531 (2016) 647–650.
[111] R. Chen, G. Romero, M.G. Christiansen, A. Mohr, P. Anikeeva, Wireless magnetothermal deep brain stimulation, Science 347 (2015) 1477–1480.
[112] R. Munshi, S.M. Qadri, Q. Zhang, I. Castellanos Rubio, P. Del Pino, A. Pralle, Magnetothermal genetic deep brain stimulation of motor behaviors in awake, freely moving mice, Elife 6 (2017), e27069.
[113] S. Rao, R. Chen, A.A. LaRocca, M.G. Christiansen, A.W. Senko, C.H. Shi, P.H. Chiang, G. Varnavides, J. Xue, Y. Zhou, S. Park, R. Ding, J. Moon, G. Feng, P. Anikeeva, Remotely controlled chemomagnetic modulation of targeted neural circuits, Nat. Nanotechnol. 14 (2019) 967–973.